International Journal of Pharmaceutics 548 (2018) 357–374

Contents lists available at ScienceDirect

International Journal of Pharmaceutics

journal homepage: www.elsevier.com/locate/ijpharm

Implication of linker length on cell cytotoxicity, pharmacokinetic and toxicity profile of gemcitabine-docetaxel combinatorial dual drug conjugate

Varun Kushwah[a,b,c], Sameer S. Katiyar[a], Ashish Kumar Agrawal[b,d,1], Isha Saraf[e], Inder Pal Singh[e], Dimitrios A. Lamprou[c,f,1], Ramesh C. Gupta[b], Sanyog Jain[a,*,2]

[a] Centre for Pharmaceutical Nanotechnology, Department of Pharmaceutics, National Institute of Pharmaceutical Education and Research, SAS Nagar, Punjab, India
[b] James Graham Brown Cancer Centre, University of Louisville, Louisville, KY, USA
[c] Strathclyde Institute of Pharmacy & Biomedical Sciences (SIPBS), University of Strathclyde, Glasgow, United Kingdom
[d] Department of Pharmaceutical Engineering and Technology, Indian Institute of Technology (IIT BHU), Varanasi, Uttar Pradesh, India
[e] Department of Natural Products, National Institute of Pharmaceutical Education and Research, SAS Nagar, Punjab, India
[f] School of Pharmacy, Queen's University Belfast, Lisburn Road, Belfast, United Kingdom

ARTICLE INFO

Keywords:
Docetaxel
Gemcitabine
Dual drug delivery
Bio-conjugation
Linker screening
Prodrug

ABSTRACT

The present study investigates effect of linkers [zero length (without linker), short length linker (glycine and lysine) and long length linker (PEG1000, PEG2000 and PEG3500)] on pharmacokinetics and toxicity of docetaxel (DTX) and gemcitabine (GEM) bio-conjugates. Conjugates were synthesized via carbodiimide chemistry and characterized by ^{1}H NMR and FTIR. Conjugation of DTX and GEM via linkers showed diverse physiochemical and plasma stability profile. Cellular uptake mechanism in MCF-7 and MDA-MB-231 cell lines revealed clathrin mediated internalization of bio-conjugates developed by using long length linkers, leading to higher cytotoxicity compared with free drug congeners. DTX-PEG3500-GEM and DTX-PEG2000-GEM demonstrated 4.21 and 3.81-fold higher $AUC_{(0-\infty)}$ of GEM in comparison with GEM alone. DTX-PEG2000-GEM and DTX-PEG3500-GEM exhibited reduced hepato-, nephro- and haemolytic toxicity as evident via histopathology, biochemical markers and SEM analysis of RBCs. Conclusively, PEG2000 and PEG3500 significantly improved pharmacokinetics without any sign of toxicity and hence can be explored further for the development of dual-drug conjugates for better therapeutic efficacy.

1. Introduction

Breast cancer is the most common malignancy in women around the world and considered as one of the most frequently observed cancer in industrialised countries. There are over 1.4 million cancer cases worldwide, 30% of which involve breast cancer with approximately 50,000 and 400 new cases in women and men, respectively, each year in the UK (Cancer Research). One third of all female cancer cases are breast cancers in India and about 1 in 8 U.S. women are supposed to be diagnosed with breast cancer in their lifetime, underscoring the need to develop an effective cancer treatment. In recent decades, the death rate in breast cancer patients has been significantly reduced due to the implementation of periodic check-ups and treatments such as chemotherapy, hormone therapy, radiotherapy, and surgery. However, there are many side effects from existing treatments; undesired off-target effects associated with high dose is the major drawback (Das et al., 2014).

To mitigate the problems associated with single chemotherapeutic drug, combination therapy of two or more therapeutic drugs came in to the picture to show the synergistic efficacy by targeting different

Abbreviations: 6-CFDA, 6-carboxyfluorescein diacetate; 8-OHdG, 8-hydroxy-2′-deoxyguanosine; AnnCy3, Annexin V-Cy3.18 conjugate; ALT, alanine transaminase; AST, aspartate transaminase; AUC, area under the curve; BUN, Blood urea nitrogen; CDA, cytidine deaminase; CDI, N,N′-Carbonyldiimidazole; CPZ, chlorpromazine; CUR, curcumin; dFdU, 2′-deoxy-2′,2′-difluorouridine; DIP, dipyridamole; DMSO, dimethyl sulfoxide; DTX, docetaxel; EDC, 1-ethyl-3-(3-dimethylaminopropyl)-carbodiimide; DSC, differential scanning calorimetry; EDTA, ethylene diamine tetra acetic acid; FBS, fetal bovine serum; GEM, gemcitabine; GNT, genistein; GLY, glycine; H&E, hematoxylin and eosin; HBBS, Hanks' Balanced Salt Solution; hCNTs, human concentrative nucleoside transporters; hENTs, human equilibrative nucleoside transporters; HLB, hydrophilic-lipophilic balance; hNTs, human nucleoside transporters; LYS, lysine; NHS, n-hydroxyl succinimide; MEM, Minimum essential medium; MDA, malondialdehyde; MTX, methotrexate; OATP, organic anion transporting polypeptide; PTX, paclitaxel; RBCs, Red blood cells

* Corresponding author.
E-mail address: sanyogjain@niper.ac.in (S. Jain).
[1] Current affiliation.
[2] ORCID: 0000-0002-0688-9563.

https://doi.org/10.1016/j.ijpharm.2018.07.016
Received 18 May 2018; Received in revised form 2 July 2018; Accepted 3 July 2018
Available online 04 July 2018
0378-5173/

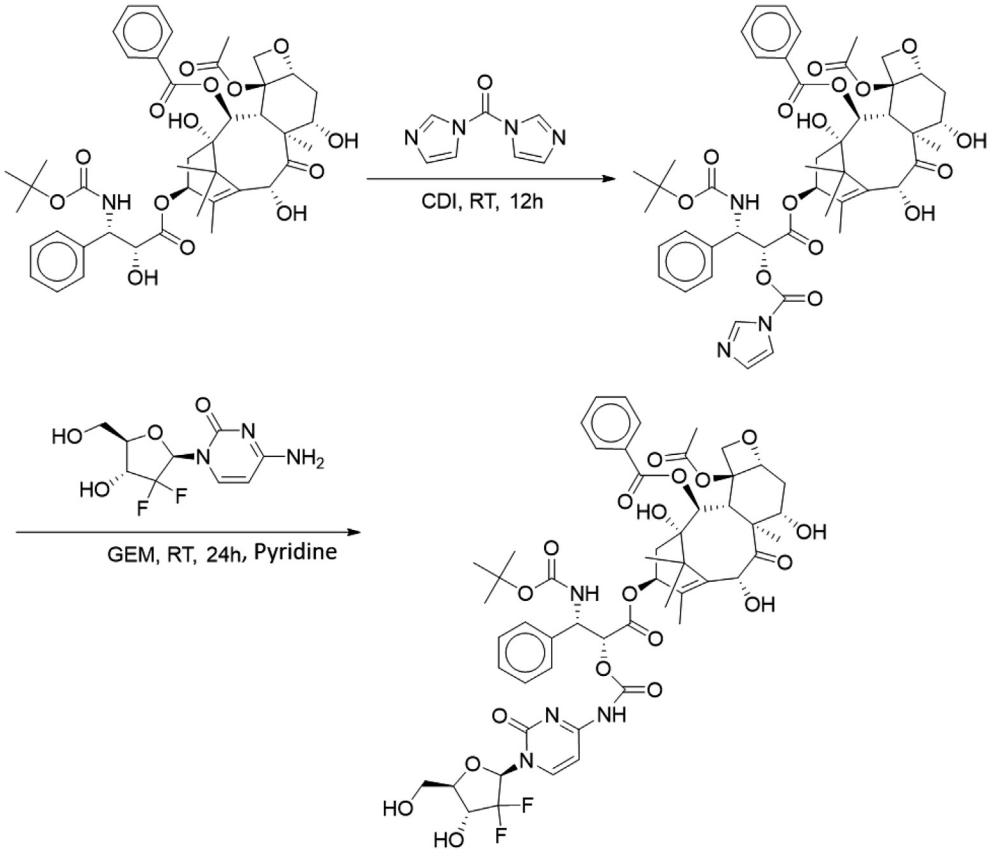

Synthesis Scheme 1. A schematic representation depicting the synthesis of DTX-GEM conjugate.

biological signalling pathways and to overcome the dose dependent side effects by reducing the dosage of each drug molecule required (Parhi et al., 2012). Moreover, combination therapy has also been emerged as a promising strategy to overcome drug resistance; as multiple chemotherapeutic drugs act through different mechanisms at different stages of the growth cycles, thereby prevents the development of drug resistance (Jain et al., 2014b). Although combination therapy has shown promising outcomes yet, unifying the pharmacokinetics of individual drugs, on-target accumulation, and intracellular uptake of various drug molecules are the major concerns which need to be addressed to get the control over dosage for maximal therapeutic effect. To circumvent these problems, variety of formulation approaches has been reported for the co-administration of drug molecules (Jain et al., 2014a; Sonawane et al., 2014; Swarnakar et al., 2014; Tan et al., 2017a; Tan et al., 2017b; Yao et al., 2014). Co-encapsulation of gambogic acid and sulforaphane in combination with DTX in PLGA based nanoparticles were reported which demonstrated significantly higher pharmacodynamic efficacy as compared to free drug combination (Huang et al., 2016; Xu et al., 2016). GEM and siRNA loaded iron oxide nanoparticles were also developed, which demonstrated enhanced bioavailability and efficacy of GEM (Li et al., 2016). However, the reports did not address the hurdle to co-deliver dual drugs with diverse physicochemical properties in a single carrier system. Dual drug conjugates of paclitaxel and GEM were reported to show higher *in vitro* cell culture cytotoxicity (Aryal et al., 2010; Caron et al., 2014) however not tested *in vivo* for efficacy.

Among the diverse formulation strategies, covalent conjugation of drugs via cleavable linkers has shown immense potential in unifying the pharmacokinetic, therapeutic efficiency and hydrophilic-lipophilic balance (HLB) of individual drug molecule (Aryal et al., 2010; Das et al., 2014; Jain et al., 2014b). Despite the positive attributes, combinatorial conjugates are still at the nascent stage of their development. In-addition, no publication is available till date, regarding screening/optimization of different bio-linkers as a tool for the development of dual drug conjugates.

To fill the lacuna, we have developed series of dual drug conjugates of GEM and DTX by using short chain linkers (Glycine, one carbon; Lysine five carbon) and long chain linkers (PEG1000, PEG2000 and PEG3500) and critically investigated the effect of different linkers on *in vitro* and *in vivo* efficacy. Both the drugs (DTX and GEM) were linked by carbamate as well as amide bond at distal ends of the linkers and was expected to exhibit pH dependent sustained release owing to controlled cleavage of the bonds. The selection of the two drugs was based upon the earlier reports in which co-administration of these two resulted in improved response rate in metastatic breast cancer, pancreatic cancer, oesophageal cancer, non-small-cell lung cancer, sarcomas, and others (Albertsson et al., 2007; Chan et al., 2009; Fidias et al., 2009; Leu et al., 2004; Sherman and Fine, 2000).

GEM is highly hydrophilic in nature (water solubility of ~38 mg/ml), with a short half-life (32–84 min) and rapidly decomposed into its inactive uracil metabolite 2′-deoxy-2′,2′-difluorouridine (dFdU), which accounts for 99% of the excreted dose (Reddy and Couvreur, 2008; Sloat et al., 2011). Consequently, frequent higher doses of GEM have to be administered to achieve the desired blood level, leading to enhanced dose dependent toxicity. On the other hand, DTX has very low water solubility (4.93 μg/ml in water) and for clinical application it is dissolved in a vehicle having high concentration of Tween 80® as solubilizer and ethanol as co-solvent, which results in severe anaphylactic (hypersensitivity) toxicity (Musumeci et al., 2006).

GEM is an inactive analogue of the nucleoside deoxycytidine and its intracellular phosphorylation yields the active di- and triphosphate metabolites. The active diphosphate form inhibits ribonucleotide reductase while the triphosphate form is incorporated into DNA which results in to the termination of DNA chain synthesis. Whereas, DTX

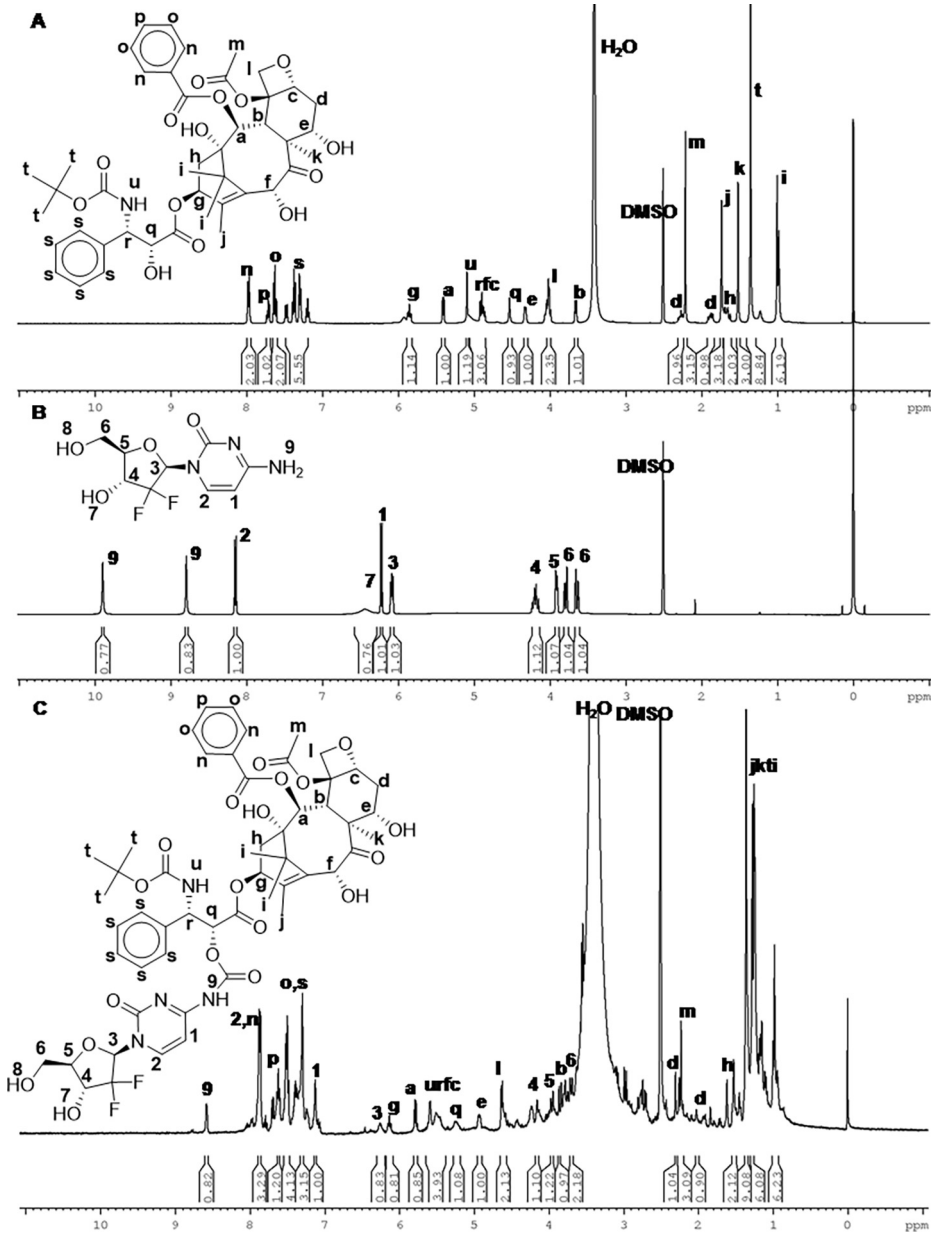

Fig. 1. [1]H NMR spectra of A: DTX; B: GEM and C: DTX-GEM Conjugate.

functions by stabilizing tubulin and induces phosphorylation of bcl-2, promoting apoptosis which results in inhibition of mitotic and interphase cellular activity. Thus the dual drug conjugate of these two drugs is expected to show the better therapeutic efficacy by targeting different pathways simultaneously providing the proper HLB balance and reduced toxicity due to less frequent dosing which are needed in case of conventional therapy.

2. Experimental section

2.1. Materials and reagents

GEM.HCL and DTX were provided as gift sample by Fresenius Kabi Oncology Limited, Gurgaon, India. Hetero bi-functional PEG1000, 2000, 3500 (NH_2-PEG-COOH) were purchased from JenKem Technology, USA. Dimethyl sulfoxide (DMSO) and dialysis membrane (1000 KD MWCO) were procured from Sigma Aldrich, USA. Pyridine, and diethyl ether were purchased from Merck, while N,N′-Carbonyldiimidazole (CDI), 1-Ethyl-3-(3-dimethylaminopropyl)-carbodiimide (EDC) and N hydroxyl succinimide (NHS) were purchased from Fluka. Minimum essential medium (MEM), fetal bovine serum (FBS), antibiotic–antimycotic solution, 3-(4,5-dimethylthiazol-2-yl)-2,5-diphenyltetrazolium bromide (MTT), Triton X-100 and ethylene diamine tetra acetic acid (EDTA) were purchased from Sigma-Aldrich Chemical Co., St. Louis, MO, USA. Pyridine was dehydrated over phosphorus pentoxide and potassium hydroxide, respectively, and distilled prior to use. MCF-7 and MDA-MB-231 cell lines were obtained American Type Culture Collection, Manassas (ATCC), VA, USA. All other solvents and reagents, unless otherwise stated, were of analytical grade and procured from local suppliers. The purity of the synthesized conjugates was determined by CHNS elemental analysis and was found to be > 95%.

2.2. Synthesis and spectral characterization of conjugates (DTX-X (linker)-GEM).

The synthesis of DTX-X-GEM conjugates was detailed in four steps as shown in synthesis schemes. These steps included: (i) Preparation of

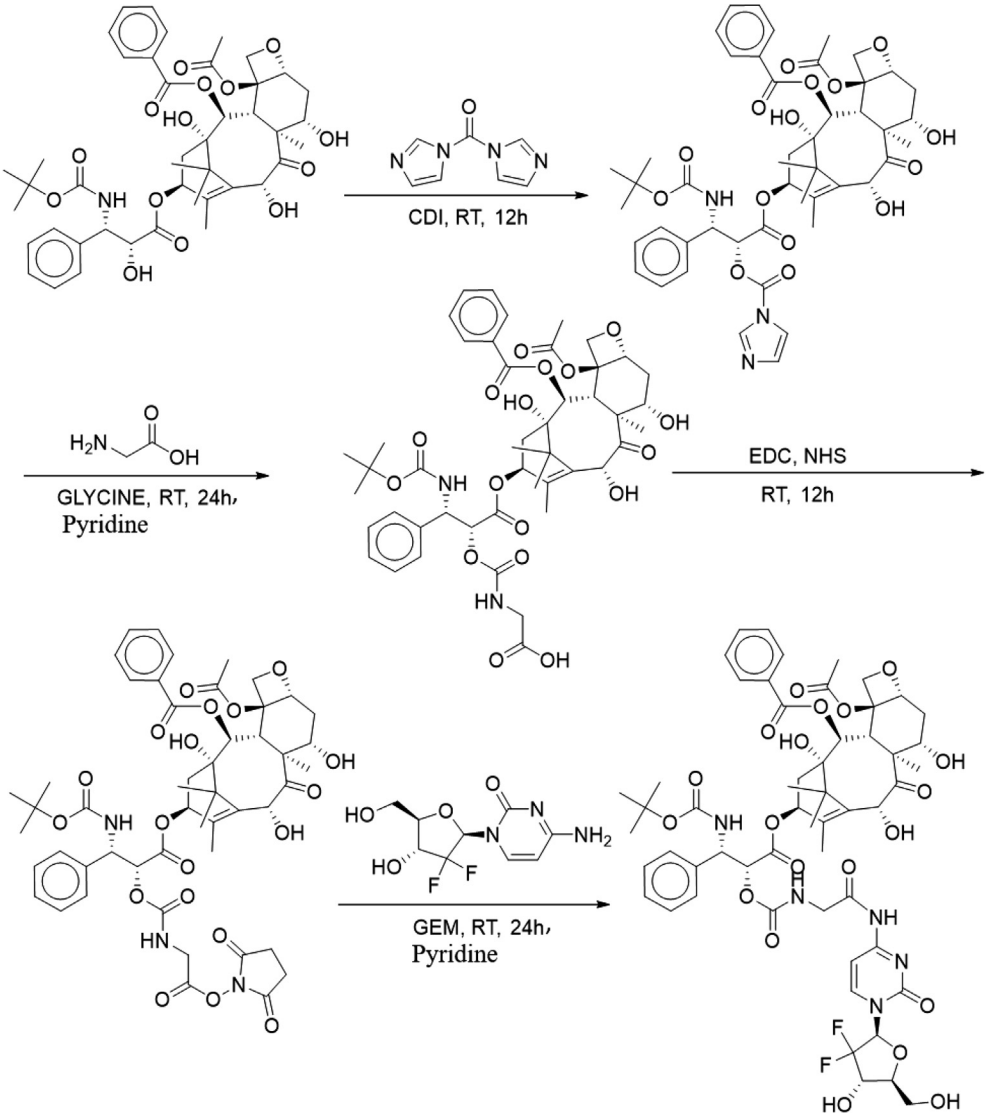

Synthesis Scheme 2. A schematic representation depicting the synthesis of DTX-GLYCINE-GEM conjugate.

active NHS ester of DTX using CDI; (ii) Conjugation of amine group of linker to the activated ester of DTX; (iii) EDC and NHS mediated activation of linker carboxylic group; (iv) Conjugation of amine group of GEM to activated ester of linker. In case of direct conjugation (without linker), DTX was activated via CDI and is directly attached to the amine group of GEM by omitting second and the penultimate steps of synthesis scheme (Synthesis Scheme 1).

The developed conjugates were then extensively characterized by complementary spectroscopic tools, i.e., FTIR, UV, NMR and elemental analysis.

^{1}H NMR of DTX (δ, DMSO-d_6, ppm, 400 MHz) (Fig. 1A)*:* 7.97 (2H, d, *J* = 7.56 Hz, H-25, H-29); 7.71 (1H, m, H-27); 7.62 (2H, m, H-26, H-28); 7.48–7.17 (5H, m, H-34, H-35, H-36, H-37, H-38); 5.85 (1H, t, *J* = 8.76 Hz, H-13); 5.40 (1H, d, *J* = 7.16 Hz, H-2); 5.09 (1H, s, 32NH); 4.92–4.85 (3H, m, H-32, H-10, H-5); 4.53 (1H, s, H-31); 4.32 (1H, d, *J* = 6.24 Hz, H-7); 4.06–3.9 (2H, m, H-20); 3.66 (1H, d, *J* = 7.08 Hz, H-3); 2.27–2.25 (1H, m, H-6); 2.21 (3H, s, H-22); 1.89–1.85 (1H, m, H-6); 1.73 (3H, s, H-18); 1.70–1.62 (2H, m, H-14); 1.51 (3H, s, H-19); 1.35 (9H, s, H-41, H-42, H-43); 0.99 (6H, m, H-16, H-17).

Elemental analysis of DTX ($C_{43}H_{53}NO_{14}$): C, 63.87; N, 1.73; H, 6.56. Found: C, 63.45; N, 1.85; H, 6.56.

^{1}H NMR of GEM.HCL (δ, DMSO-d_6, ppm, 400 MHz) (Fig. 1B)*:* 9.89 (1H, s, 4′NH_2); 8.79 (1H, s, 4′NH_2); 8.14 (1H, d, *J* = 7.88 Hz, H-6′); 6.43 (1H, s, 3″OH); 6.22 (1H, d, *J* = 7.88 Hz, H-5′); 6.08 (1H, m, H-1″); 4.23–4.15 (1H, m, H-3″); 3.92–3.90 (1H, m, H-4″); 3.80–3.77 (1H, d, *J* = 12.36 Hz, H-5″); 3.66–3.62 (1H, dd, *J* = 12.76 Hz, 3.36 Hz, H-5″).

Elemental analysis of GEM ($C_9H_{12}N_3O_4ClF_2$): C, 36.04; N, 14.01; H, 4.67. Found: C, 36.18; N, 14.1; H, 4.56.

2.2.1. Synthesis of activated DTX

Activated DTX was synthesized via carbodiimide chemistry by dissolving DTX (100 mg, 0.123 mM) in 5 ml DMSO and further activated by adding stoichiometric molar equivalent of CDI at room temperature under constant stirring of 300 rpm for 24 h. The mixture was filtered and poured drop wise into ice cold diethyl ether to precipitate activated DTX and to remove the imidazole by product.

2.2.2. Synthesis of intermediate DTX-linker(s)

Activated DTX (100 mg, 0.11 mM) and 0.11 mM Linker (glycine, 8.25 mg; lysine, 16.17 mg; PEG1000, 110 mg; PEG2000, 220 mg and PEG3500, 385 mg) were dissolved in 5 ml DMSO in the presence of pyridine and allowed to react at room temperature under constant stirring of 300 rpm for 24 h. The reaction mixture was then filtered and poured drop wise to ice cold diethyl ether to precipitate the developed DTX-linker conjugate as well as to remove free imidazole. The precipitate was separated via decantation and further dried.

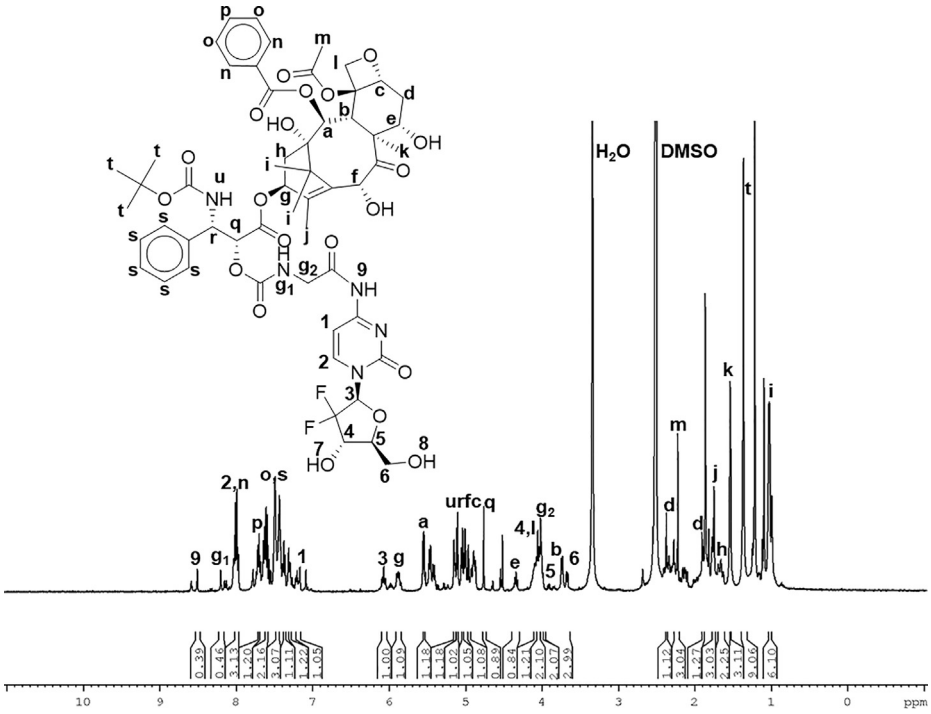

Fig. 2. ^{1}H NMR spectrum of DTX-GLYCINE-GEM conjugate.

2.2.3. Synthesis of DTX-GEM (without linker)

DTX was activated first via CDI and then the activated DTX was further conjugated by GEM (Synthesis Scheme 1). Briefly, the activated DTX (100 mg, 0.11 mM) was dissolved in 4 ml DMSO and reacted with GEM (29 mg, 0.11 mM dissolved in 1 ml of DMSO) at room temperature for 24 h in the presence of pyridine. Again, the reaction mixture was filtered and added drop wise to ice cold diethyl ether to obtain DTX-GEM conjugate. Thereafter, the conjugate was purified via dialysis membrane with molecular weight cut-off of 1000 and freeze dried.

2.2.3.1. Docetaxel-gemcitabine conjugate (DTX-GEM). State of aggregation: White solid; Yield: 68.6%

UV Vis (λ_{max}, nm): 228, 272

^{1}H NMR (δ, DMSO-d_6, ppm, 400 MHz) (Fig. 1C): 8.58 (1H, s, 4′NH); 7.86 (3H, m, H-6′, H-25, H-29); 7.70–7.24 (8H, m, H-26 to H-28 and H-34 to H-38); 7.12–7.08 (1H, m, H-5′); 6.47 (1H, m, H-1″); 6.13 (1H, t, J = 8.56 Hz, H-13); 5.78 (1H, d, J = 7.48 Hz, H-2); 5.58 (1H, s, 32NH); 5.50–5.45 (3H, m, H-32, H-10, H-5); 5.25 (1H, s, H-31); 4.92 (1H, d, J = 6.12 Hz, H-7); 4.63–4.54 (2H, m, H-20); 4.23–4.12 (1H, m, H-3″); 4.03–3.94 (1H, m, H-4″); 3.85 (1H, m, H-3); 3.77–3.68 (2H, m, H-5″); 2.30–2.25 (1H, m, H-6); 2.22 (3H, s, H-22); 2.02–1.90 (1H, m, H-6); 1.61–1.44 (2H, m, H-14); 1.35–0.97 (21H, m, H-18, H-19, H-41, H-42, H-43, H-16, H-17).

Elemental analysis of DTX-GEM ($C_{53}H_{65}N_4O_{19}F_2$): C, 57.97; N, 5.10; H, 5.92. Found: C, 57.83; N, 5.02; H, 5.79.

2.2.4. Synthesis of DTX-X-GEM

Activated DTX was conjugated to amine group of short chain (glycine and lysine) and long chain linkers (bi-functionalized PEG1000, PEG2000 and PEG3500). Further, the carboxyl group of linkers was activated by EDC/NHS and reacted with GEM to form final DTX-X-GEM conjugate. Briefly, 0.11 mM DTX linker (DTX-glycine, DTX-lysine, DTX-PEG1000, DTX-PEG2000 and DTX-PEG3500) was dissolved in 5 ml DMSO and the free carboxyl group of the DTX-linker group was activated by EDC/NHS (1:1.2 mol ratio of DTX-linker and EDC/NHS) in the presence of pyridine. After 24 h, the mixture was precipitated in ether to separate unreacted EDC/NHS and then dissolved again in 5 ml DMSO and reacted with free GEM.HCL (29 mg, 0.11 mM). The reaction mixture was filtered and the final conjugate was then precipitated in diethyl ether and further separated by decantation. Thereafter, the conjugates were dialysed using molecular weight cut off of 1000, 1500, 2500 and 4000 for non-PEGylated linkers (DTX-GLY-GEM and DTX-LYS-GEM), DTX-PEG1000-GEM, DTX-PEG2000-GEM and DTX-PEG3500-GEM conjugate, respectively, and freeze dried.

2.2.4.1. Docetaxel-glycine-gemcitabine conjugate (DTX-GLY-GEM; Synthesis Scheme 2). State of aggregation: White solid; Yield: 65.7%.

UV Vis (λ_{max}, nm): 228, 272

^{1}H NMR (δ, DMSO-d_6, ppm, 400 MHz) (Fig. 2): 8.50 (1H, s, 4′NH); 8.20 (1H, s, 2‴NH); 8.02–7.96 (3H, m, H-6′, H-25, H-29); 7.77–7.29 (8H, m, H-26 to H-28 and H-34 to H-38); 7.20–7.16 (1H, m, H-5′); 6.06 (1H, t, J = 8.12 Hz, H-1″); 5.87 (1H, m, H-13); 5.55 (1H, d, J = 7.12 Hz, H-2); 5.14–4.86 (4H, m, 32NH, H-32, H-10, H-5); 4.75 (1H, s, H-31); 4.33 (1H, m, H-7); 4.08–3.98 (5H, m, H-3‴, H-20 and H-2‴); 3.91–3.65 (4H, m, H-4‴, H-3 and H-5‴); 2.36–2.35 (1H, m, H-6); 2.21 (3H, s, H-22); 1.90–1.88 (1H, m, H-6); 1.74 (3H, s, H-18): 1.68–1.62 (2H, m, H-14); 1.53 (3H, s, H-19); 1.36 (9H, s, H-41, H-42, H-43); 1.02–1.01 (6H, m, H-16, H-17).

Elemental analysis of DTX-GLY-GEM ($C_{55}H_{69}N_5O_{20}F_2$): C, 57.13; N, 6.06; H, 5.97. Found: C, 57.19; N, 6.18; H, 5.85.

2.2.4.2. Docetaxel-lysine-gemcitabine conjugate (DTX-LYS-GEM; Synthesis Scheme 3). State of aggregation: White solid; Yield: 64.2%.

UV Vis (λ_{max}, nm): 228, 272

^{1}H NMR (δ, DMSO-d_6, ppm) (Fig. 3): 8.50 (1H, s, 4′NH); 8.10 (1H, s, 6‴NH); 8.02–7.96 (3H, m, H-6′, H-25, H-29); 7.77–7.29 (8H, m, H-26 to H-28 and H-34 to H-38); 7.21–7.16 (1H, m, H-5′); 6.06 (1H, t, J = 8.92 Hz, H-1″); 5.88 (1H, m, H-13); 5.53 (1H, d, J = 7.12 Hz, H-2); 5.14–4.86 (4H, m, 32NH, H-32, H-10, H-5); 4.75 (1H, s, H-31); 4.45 (2H, m, H-6‴); 4.33 (1H, m, H-7); 4.07–4.01 (3H, m, H-3″ and H-20); 3.92–3.65 (4H, m, H-4″, H-3 and H-5″); 3.57–3.51 (1H, m, H-2‴); 2.36–2.35 (1H, m, H-6); 2.21 (3H, s, H-22); 1.90–1.88 (1H, m, H-6); 1.82–1.81 (2H, m, H-3‴); 1.74 (3H, s, H-18): 1.68–1.62 (2H, m, H-14); 1.53 (3H, s, H-19); 1.35 (9H, s, H-41, H-42, H-43); 1.02–1.01 (6H, m, H-16, H-17).

Elemental analysis of DTX-LYS-GEM ($C_{59}H_{78}N_6O_{20}F_2$): C, 57.73; N,

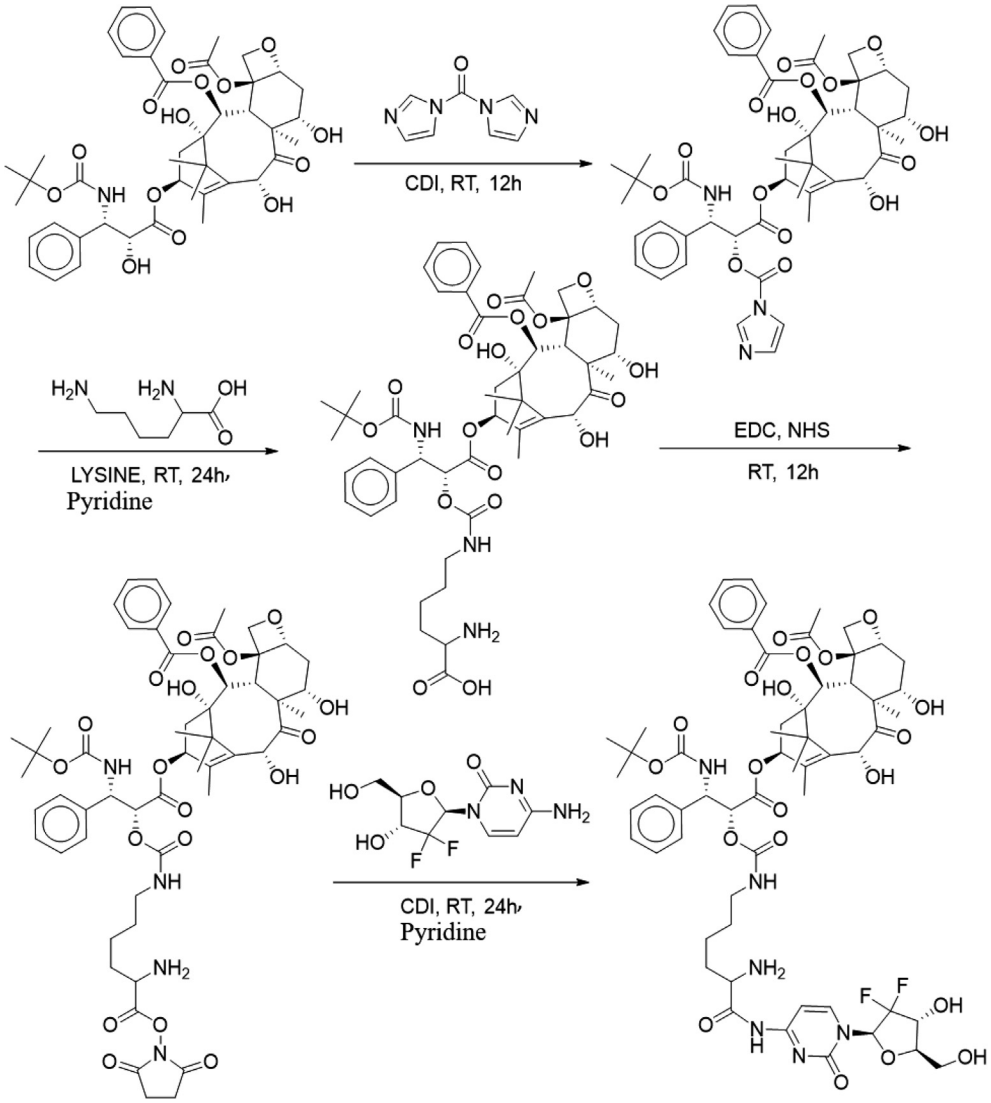

Synthesis Scheme 3. A schematic representation depicting the synthesis of DTX-LYS-GEM conjugate.

6.85; H, 6.36. Found: C, 57.59; N, 6.89; H, 6.45.

2.2.4.3. Docetaxel-PEG1000-gemcitabine conjugate (DTX-PEG1000-GEM; Synthesis Scheme 4). State of aggregation: White solid; Yield: 65.2%.

UV Vis (λ_{max}, nm): 228, 272.

^{1}H NMR (δ, DMSO-d_6, ppm) (Fig. 4A): 8.50 (1H, s, 4′NH); 8.08 (1H, s, NH of PEG); 8.00–7.96 (3H, m, H-6′, H-25, H-29); 7.73–7.29 (8H, m, H-26 to H-28 and H-34 to H-38); 7.19–7.16 (1H, m, H-5′); 6.06 (1H, t, J = 8.12 Hz, H-1″); 5.87 (1H, m, H-13); 5.54 (1H, d, J = 7.12 Hz, H-2); 5.14–4.86 (4H, m, 32NH, H-32, H-10, H-5); 4.75 (1H, s, H-31); 4.33 (1H, m, H-7); 4.06–4.00 (3H, m, H-3″ and H-20); 3.95–3.89 (1H, m, H-4″); 3.87 (2H, t, CH_2 protons of PEG); 3.74–3.72 (1H, d, H-3); 3.69–3.65 (2H, m, H-5″); 3.51 (CH2-CH2-O-, t, protons of PEG); 2.33–2.32 (1H, m, H-6); 2.21 (3H, s, H-22); 1.90–1.88 (1H, m, H-6); 1.74 (3H, s, H-18): 1.68–1.62 (2H, m, H-14); 1.53 (3H, s, H-19); 1.35 (9H, s, H-41, H-42, H-43); 1.02–1.01 (6H, m, H-16, H-17).

Elemental analysis of DTX-PEG1000-GEM ($C_{97}H_{151}N_5O_{41}F_2$): C, 56.01; N, 3.36; H, 7.26. Found: C, 56.14; N, 3.47; H, 7.29.

2.2.4.4. Docetaxel-PEG2000-gemcitabine conjugate (DTX-PEG2000-GEM; Synthesis Scheme 4). State of aggregation: White solid; Yield: 62.6%

UV Vis (λ_{max}, nm): 228, 272

^{1}H NMR (δ, DMSO-d_6, ppm) (Fig. 4B): 8.50 (1H, s, 4′NH); 8.08 (1H, s, NH of PEG); 8.00–7.96 (3H, m, H-6′, H-25, H-29); 7.73–7.29 (8H, m, H-26 to H-28 and H-34 to H-38); 7.19–7.16 (1H, m, H-5′); 6.06 (1H, t, J = 8.12 Hz, H-1″); 5.87 (1H, m, H-13); 5.54 (1H, d, J = 7.12 Hz, H-2); 5.14–4.86 (4H, m, 32NH, H-32, H-10, H-5); 4.75 (1H, s, H-31); 4.33 (1H, m, H-7); 4.06–4.00 (3H, m, H-3″ and H-20); 3.95–3.89 (1H, m, H-4″); 3.87 (2H, t, CH_2 protons of PEG); 3.74–3.72 (1H, d, H-3); 3.69–3.65 (2H, m, H-5″); 3.51 (CH2-CH2-O-, t, protons of PEG); 2.33–2.32 (1H, m, H-6); 2.21 (3H, s, H-22); 1.90–1.88 (1H, m, H-6); 1.74 (3H, s, H-18): 1.68–1.62 (2H, m, H-14); 1.53 (3H, s, H-19); 1.35 (9H, s, H-41, H-42, H-43); 1.02–1.01 (6H, m, H-16, H-17).

Elemental analysis of DTX-PEG2000-GEM ($C_{143}H_{243}N_5O_{64}F_2$): C, 55.53; N, 2.26; H, 7.86. Found: C, 55.67; N, 2.41; H, 7.78.

2.2.4.5. Docetaxel-PEG3500-gemcitabine conjugate (DTX-PEG3500-GEM; Synthesis Scheme 4). State of aggregation: White solid; Yield: 66.4%

UV Vis (λ_{max}, nm): 228, 272

^{1}H NMR (δ, DMSO-d_6, ppm) (Fig. 4C): 8.50 (1H, s, 4′NH); 8.08 (1H, s, NH of PEG); 8.00–7.96 (3H, m, H-6′, H-25, H-29); 7.73–7.29 (8H, m, H-26 to H-28 and H-34 to H-38); 7.19–7.16 (1H, m, H-5′); 6.06 (1H, t, J = 8.12 Hz, H-1″); 5.87 (1H, m, H-13); 5.54 (1H, d, J = 7.12 Hz, H-2); 5.14–4.86 (4H, m, 32NH, H-32, H-10, H-5); 4.75 (1H, s, H-31); 4.33 (1H, m, H-7); 4.06–4.00 (3H, m, H-3″ and H-20); 3.95–3.89 (1H, m, H-4″); 3.87 (2H, t, CH_2 protons of PEG); 3.74–3.72 (1H, d, H-3); 3.69–3.65

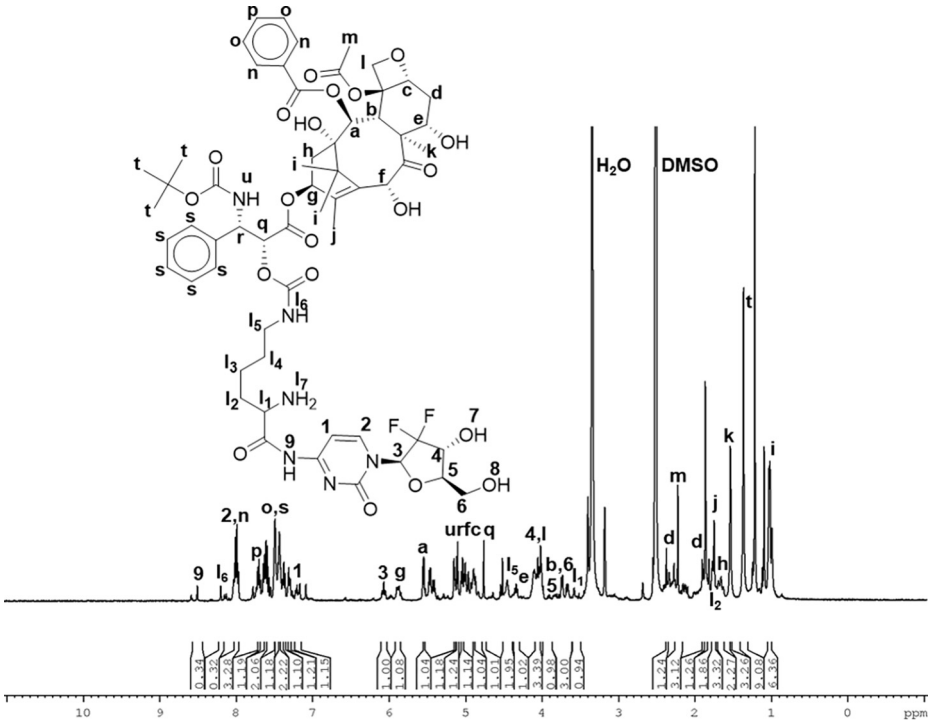

Fig. 3. ^{1}H NMR spectra of DTX-LYSINE-GEM conjugate.

(2H, m, H-5″); 3.51 (CH2-CH2-O-, t, protons of PEG); 2.33–2.32 (1H, m, H-6); 2.21 (3H, s, H-22); 1.90–1.88 (1H, m, H-6); 1.74 (3H, s, H-18): 1.68–1.62 (2H, m, H-14); 1.53 (3H, s, H-19); 1.35 (9H, s, H-41, H-42, H-43); 1.02–1.01 (6H, m, H-16, H-17).

Elemental analysis for DTX-PEG3500-GEM ($C_{211}H_{379}N_5O_{98}F_2$): C, 55.21; N, 1.52; H 8.26. Found: C, 55.10; N, 1.61; H, 8.12.

2.3. In vitro hydrolysis in simulated fluids

In vitro hydrolysis of DTX-X-GEM conjugates was evaluated by analyzing the rate of GEM release in phosphate buffered saline (PBS) of pH 5.5 and pH 7.4, in the presence and absence of protease in order to simulate the tumor microenvironment and systemic circulation, respectively (Das et al., 2014). Briefly, synthesized conjugates, equivalent to 1 mg GEM, dissolved in 1 ml of the distilled water (containing 20 µl of 5 U/ml concentration of enzyme) were taken in a dialysis bag (molecular weight cutoff 500 Da) and placed in 5 ml of media. At scheduled time intervals, samples aliquots (1 ml) were withdrawn and replaced with the equal amount of fresh media to maintain the sink conditions. The free GEM content released from the conjugates was then analyzed by validated HPLC method.

2.4. Plasma stability studies

In vitro degradation of GEM from the synthesized conjugates (equivalent to 0.5 mg GEM) into the metabolite (2′,2′-difluorodeoxyuridine (dFdU)) was measured by incubating free GEM.HCL and conjugates in plasma (1 ml) for 24 h at 37 °C. At predetermined time intervals, samples were withdrawn and analyzed by validated bioanalytical method using HPLC (Lin et al., 2004).

2.5. In vitro cell culture experiments

2.5.1. Cells

In vitro cell culture experiments were performed in Human breast cancer cell lines (MCF-7 and MDA-MB-231; American Type Culture Collection, Manassas (ATCC), VA, USA). Media and culture conditions were utilized for the growth of MCF-7 and MDA-MB-231 cell lines as per ATCC protocols. The cultured cells were trypsinized once 90% confluent with 0.25% trypsin-EDTA solution and seeded at a density of 50,000 cells/well in 6-well culture plate (Costars, Corning Inc., NY, USA) for cell uptake and apoptosis analysis. Moreover, MTT assay was also employed to determine the cell viability of MCF-7 and MDA-MB-231 cells by seeding in 96-well cell culture plates (Costars, Corning Inc., NY, USA) at a density 10,000 cells/well.

2.5.2. In vitro cytotoxicity assay

MTT assay was employed to determine the cell cytotoxicity of samples in MCF-7 and MDA-MB-231 cell lines, following our previously reported protocol (Dora et al., 2016). Briefly, both the cell lines were seeded to 96-well tissue culture plates and kept overnight. Following the attachment of cells, fresh medium containing free GEM, DTX, combination of GEM and DTX (1:1 M ratio) and synthesized conjugates were added at concentrations of 0.1, 1, 10, and 20 µg/ml (equivalent to free DTX). After the incubation period of 24, 48 and 72 h, the medium was aspirated and the viability of the cells was measured by solubilizing the formazan crystals with DMSO and the optical density (OD) of the resultant solution was then measured at 540 nm using an ELISA plate reader (BioTek, USA). The cell viability was calculated using Eq. (1):

$$Relative\ \ cell\ \ viability = \frac{Absorbance\ \ (Sample)}{Absorbance\ \ (Control)} \quad (1)$$

2.5.3. DNA damage assay

The DNA damage potential of the developed conjugates was assessed as a function of alterations in 8-hydroxyguanosine (8-OHdG) levels. Briefly, MCF-7 and MDA-MB-231 cells were exposed to different samples at 10 µg/ml equivalent to DTX for 24 h. Cells were then washed with HBSS and 8-OHdG level within the cells was estimated. DMSO treated cells were employed as negative control.

2.5.4. Cell uptake and internalization pathway

Dipyridamole was utilized as transporter inhibitor, to evaluate the hNTs and OATP dependent membrane permeation of free drugs and

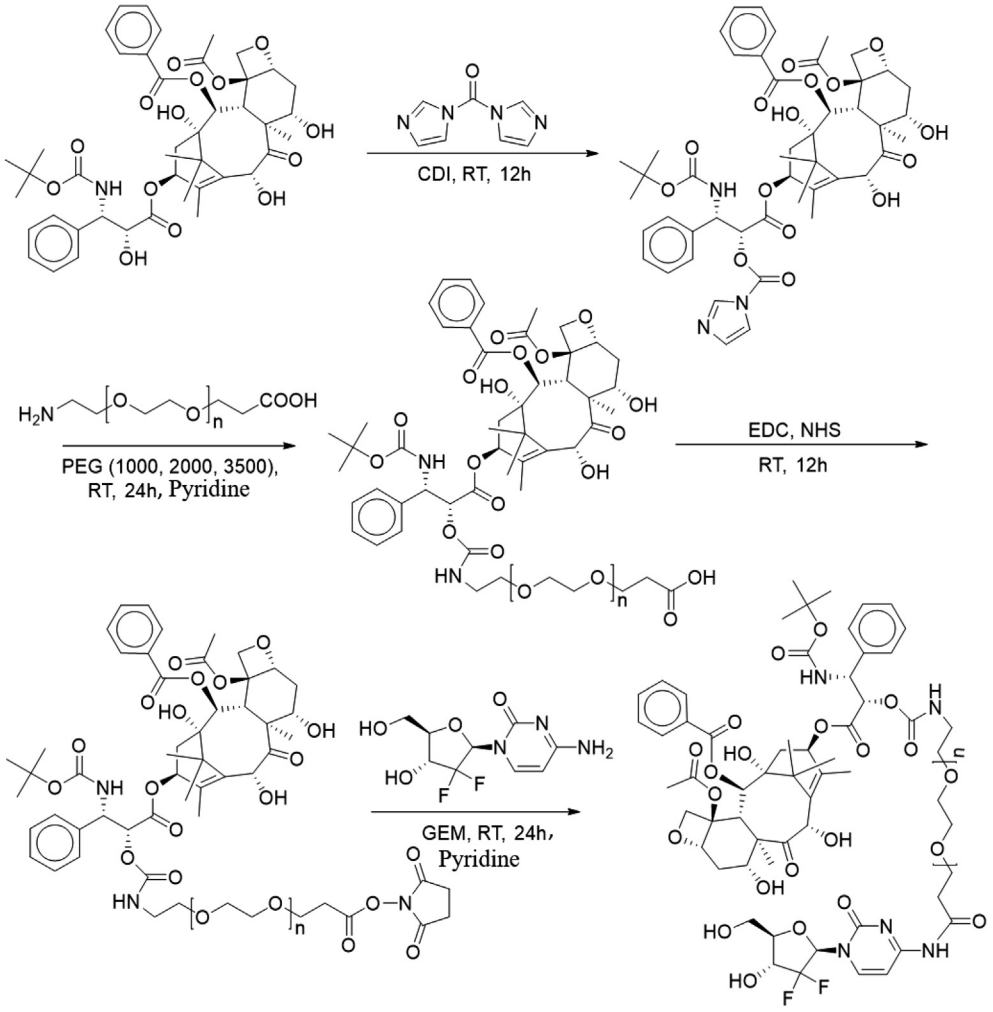

Synthesis Scheme 4. A schematic representation depicting the synthesis of DTX-PEG (1000, 2000, 3500)-GEM conjugates.

conjugates (Karlgren et al., 2012; Liu et al., 2014; Mackey et al., 1998). In addition, the internalization pathway of conjugates was evaluated by incubating endocytotic inhibitors, *viz.* genistein (GNT, caveolae mediated endocytosis inhibitor), chlorpromazine (CPZ, clathrin mediated endocytosis inhibitor) and combined treatment of CPZ and GNT. Briefly, MCF-7 and MDA-MB-231 (10,000 cells/well) were seeded in 96-well plates and incubated with inhibitors *viz.* dipyridamole (DIP) (10 mM, hNTs and OATP transporter inhibitor), GNT (50 μg/ml) and CPZ (20 μg/ml) for 1 h. Following the incubation, the media was aspirated and the cells were incubated with free drugs, their combination (1:1 M ratio) and synthesized conjugates at concentrations of 0.1, 1, 5, and 10 μg/ml (equivalent to free DTX) for 24 h and IC_{50} was calculated by CalcuSyn 2.1 software.

2.5.5. Subcellular fate of free drug and conjugates

The intracellular localization of free drugs and conjugates was evaluated using lysosome specific dye LysoTracker (Ex/Em 577/590 nm). Briefly, MCF-7 and MDA-MB-231 were treated with the free drugs and the conjugates at a concentration of 10 μg/ml (equivalent to free DTX) for 24 h. Following treatment, the cells were washed with HBSS. The cells were then incubated with LysoTracker Red (1 μM) for 30 min in dark at 37 °C. Thereafter, the cells were washed thrice using HBSS to remove the excess dye. After washing the cells were fixed using 2.5% glutaraldehyde solution and were observed under a confocal laser microscope (CLSM) (Olympus FV1000).

2.5.6. Annexin V apoptosis assay

The *in vitro* apoptosis was evaluated in MCF-7 and MDA-MB-231 cells to further assess the cytotoxic potential, via standard phosphatidyl serine externalization assay based on Annexin V binding. Briefly, MCF-7 and MDA-MB-231 cells were incubated with fresh media containing samples, equivalent to 10 μg/ml DTX, for 6 h. After incubation, the cells were washed thrice with HBSS and stained with Annexin V-Cy3.18 conjugate (AnnCy3) and 6-carboxyfluorescein diacetate (6-CFDA) following the manufacturer's protocol (Annexin V-Cy3™ Apoptosis Detection Kit, Sigma, USA) and were observed by CLSM under green and red channels for 6-CFDA and AnnCy3, respectively. The cells stained with green and red fluorescence were considered as live and necrotic, respectively, while, those stained with both red and green were regarded as apoptotic. Further, apoptotic index was calculated as a ratio of red fluorescence (originated from the Annexin V Cy3.18 conjugate, measure of apoptosis) to that of green fluorescence (originated from the 6-carboxyfluorescein, measure of viable cells) as an qualitative estimation of apoptosis, while, quantitative measure of fluorescence within the images was measured by using Image J software (U. S. National Institutes of Health, Bethesda, Maryland, USA, http://imagej.nih.gov/ij/).

2.6. In vivo pharmacokinetics

2.6.1. Animals and dosing

Female Sprague Dawley (SD) rats of 220–230 g were supplied by the central animal facility, National Institute of Pharmaceutical Education

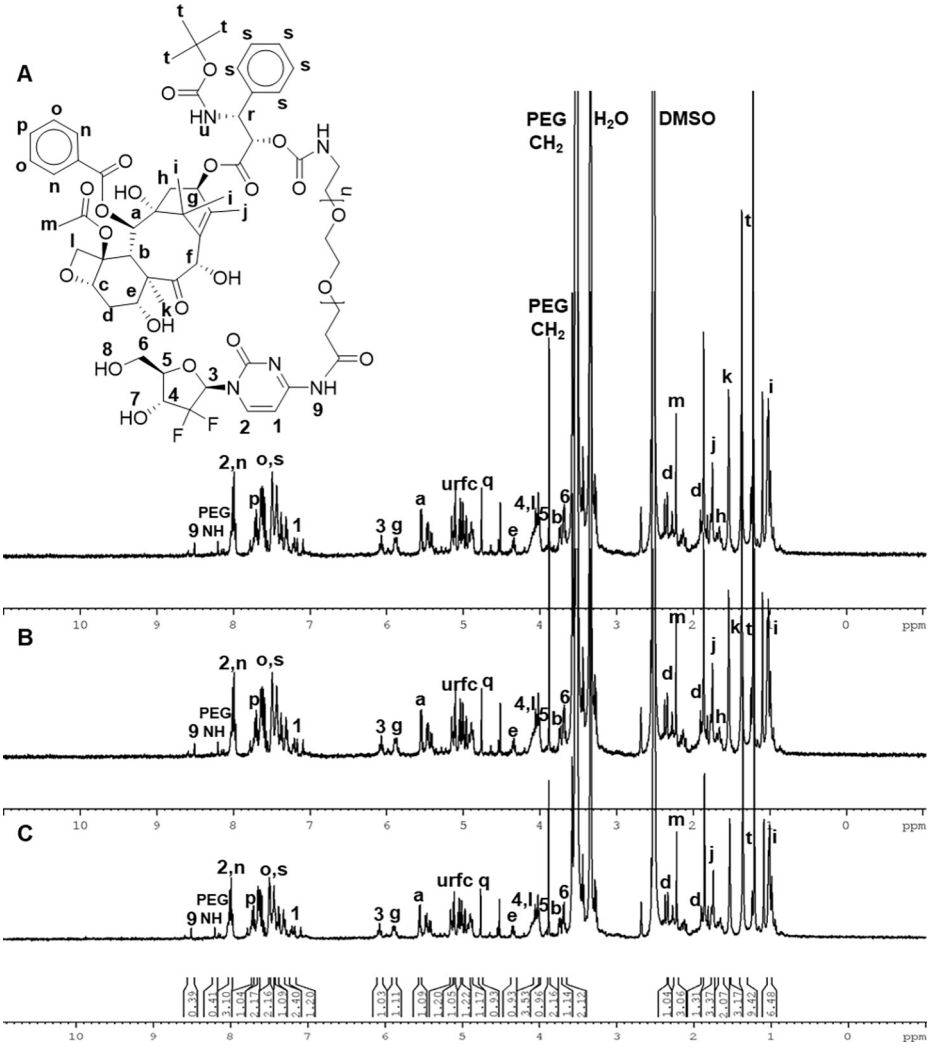

Fig. 4. ^{1}H NMR spectrum of A: DTX-PEG(1000)-GEM; B: DTX PEG(2000)-GEM and C: DTX-PEG(3500)-GEM.

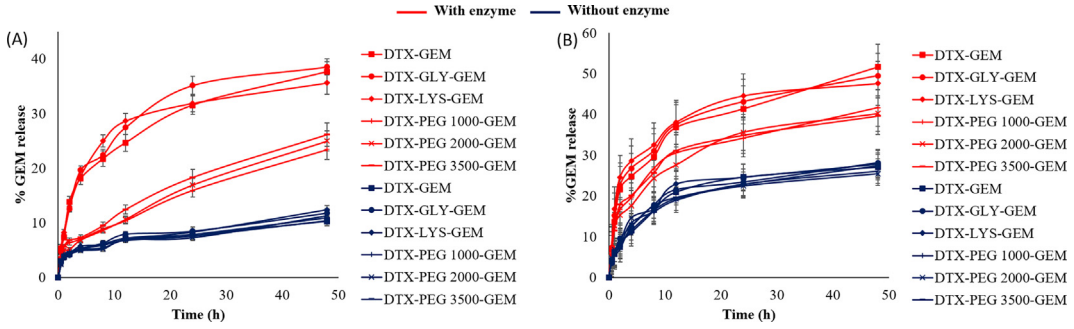

Fig. 5. In-vitro release of conjugates at pH (A) 7.4 and (B) 5.5 in the absence and presence of proteases.

& Research (NIPER), India following the approval of all the animal protocols by the Institutional Animal Ethics Committee (IAEC). Prior to experiments, the animals were acclimatized at temperature of 25 ± 2 °C and relative humidity of 50–60% under natural light/dark conditions for 1 week. Thereafter, the animals were randomly distributed into different groups each containing 5 animals. 1st group (control) of animals received marketed formulation of GEM (Gemzar®), while, 2nd to 7th groups received DTX-GEM, DTX-GLY-GEM, DTX-LYS-GEM, DTX-PEG1000-GEM, DTX-PEG2000-GEM and DTX-PEG3500-GEM, respectively. All the samples were administered via tail vein at a dose equivalent to 10 mg/kg GEM. The blood samples (approximately 0.2 ml) were collected from the tail vein into the micro centrifuge tubes containing heparin (40 IU/ml of blood). Plasma and RBCs were separated by centrifuging the blood samples at 3000 rcf for 5 min at 4 °C. To 100 µl of plasma, 200 µl of acetonitrile was added to precipitate proteins and again centrifuged at 10,000 rpm for 10 min at 4 °C. The supernatant was separated and analyzed for GEM content by validated HPLC method (Vandana and Sahoo, 2010; Vergniol et al., 1992).

2.6.2. Pharmacokinetic data analysis

The pharmacokinetic data was analysed by one compartmental model, using Kinetica software (Thermo scientific). Required

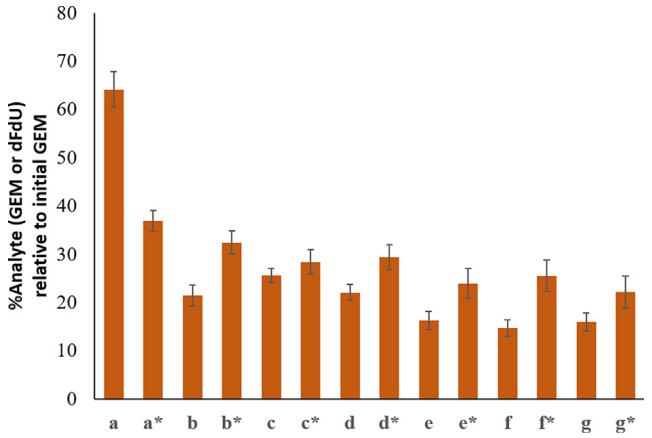

Fig. 6. Percent of dFdU and GEM (*) following incubation of (a) free GEM, (b) DTX-GEM, (c) DTX-GLY-GEM, (d) DTX-LYS-GEM, (e) DTX-PEG1000-GEM, (f) DTX-PEG2000-GEM and (g) DTX-PEG3500-GEM in the presence of plasma. Values are expressed as Mean ± SD (n = 3).

pharmacokinetics parameters like total area under the curve $(AUC)_{0-\infty}$, terminal phase half-life ($t_{1/2}$), peak plasma concentration (C_{max}) and time to reach the maximum plasma concentration (T_{max}) were determined.

2.6.3. Toxicity evaluation

After 7 days of treatment, the animals were sacrificed and blood was collected by cardiac puncture and the separated plasma was then analyzed for various toxicity markers *viz.* alanine transaminase (ALT), aspartate transaminase (AST), Blood urea nitrogen (BUN) and creatinine by commercially available diagnostic kits (Accurex Pvt. Ltd., India). From the same group of animals, liver was isolated and homogenized in 5 volumes of PBS (pH 7.4) for the estimation of oxidative stress marker, malondialdehyde (MDA). In addition, liver, kidney and spleen tissues, excised from each group, were processed as per the routine protocol and further stained with hematoxylin and eosin (H&E) for histopathological evaluations.

2.6.4. In vivo hemolysis

The effect on Red Blood Cells (RBCs) following the sample treatment was accessed to analyze real hematotoxicity profile in *in vivo* conditions. Briefly, after 7 days of treatment, RBCs pellet was collected, as per the procedure mentioned above in Section 2.6.1, and suspended in 0.5% glutaraldehyde in phosphate buffer (pH 7.4) for 60 min and further washed five times with distilled water. Finally, fixed RBCs were dispersed and imaged under SEM.

2.7. Statistical analysis

All the data are expressed as mean ± standard deviation (SD) and mean ± standard error of mean (SEM) for all *in vitro* and *in vivo* results, respectively. Statistical analysis was performed using Sigma Stat (version 3.5) utilizing one-way ANOVA followed by Tukey–Kramer multiple comparison test. $p < 0.05$ was considered as statistically significant difference.

3. Results

3.1. In vitro hydrolysis in simulated media

The *in vitro* hydrolysis of the synthesized conjugates (DTX-X-GEM) was evaluated at pH 5.5 and 7.4 with or without protease enzyme. As evident from the Fig. 5, the synthesized conjugates exhibited nominal amount of hydrolysis at pH 7.4 without protease, however, the same was increased at pH 5.5. Interestingly, conjugates synthesized with zero and short linker exhibited significantly higher rate of release indicating less stability towards enzymatic hydrolysis, while, addition of protease enzyme at different pH barely influenced the rate of GEM release from the conjugates synthesized from long linkers.

3.2. Plasma stability studies

The plasma stability of GEM in case of different conjugates was evaluated by estimating the percentage of free GEM and its metabolite (dFdU) with time. It is evident from the Fig. 6 that free GEM showed rapid degradation into its inactive metabolite, while, the synthesized conjugates demonstrated remarkably higher stability of GEM against the enzymatic degradation. In case of free GEM, ~64% of the metabolite (dFdU) was detected, while short chain linkers and long chain linkers demonstrated approximately 22 and 15% of the dFdU level, respectively, following the 24 h incubation in plasma, indicative of higher stability of GEM in case of PEGylated conjugates.

3.3. In vitro cell culture experiments

3.3.1. In vitro cytotoxicity assay

The cell cytotoxicity results (Fig. 7(I and II)) revealed higher sensitivity in case of MDA-MB-231 compared to MCF-7 cell lines when treated with the conjugates. Furthermore, significantly higher cell cytotoxicity was found in case of DTX-PEG2000-GEM as compared to free drugs, and conjugates with short chain linker (Table 1, control group). Interestingly, the conjugates with short length linker showed even lower cell cytotoxicity as compared to free GEM and DTX combination.

3.3.2. DNA damage assay

The DNA damage assay revealed that observed cytotoxicity of the free drug and conjugates is mediated by DNA damage. Significantly higher levels of 8-OHdG were observed in case of long length linker conjugates as compared to free drugs, zero and short linker conjugates. Among the long length linker conjugates, DTX-PEG2000-GEM exhibited higher levels of 8-OHdG in comparison with DTX-PEG1000-GEM and DTX-PEG3500-GEM (Fig. 7(III)).

3.3.3. Cell uptake and internalization pathway

Selective transporter inhibition assay was performed to investigate the dependence mechanism of free drugs and conjugates on the hNTs (transporter for GEM) and OATP (transporter for DTX) for their therapeutic effect. MCF-7 and MDA-MB-231 cell lines were pre-incubated with dipyridamole (hNTs and OATP inhibitor), thereafter, the cells were treated with different concentrations of samples for 24 h and IC_{50} values were obtained. MCF-7 and MDA-MB-231 exhibited 6.30 and 6.87-folds higher IC_{50} value in case of DTX, while, 10.60 and 8.83-fold resistance in case of GEM treatment, respectively, on pre-incubation of cells with dipyridamole (DIP) as compared to cells devoid of DIP. Noteworthy, the zero and short length linker also demonstrated higher resistance, while, in case of long length linker conjugates, an insignificant difference in IC_{50} value was observed, in both the cell lines on pre-treatment with DIP. Pre-incubation of cells with GNT and CPZ demonstrated almost no effect on IC_{50} in case of zero and short length linker while IC_{50} of DTX-PEG1000-GEM, DTX-PEG2000-GEM and DTX-PEG3500-GEM conjugates, was found to be significantly increased in both the cell lines (Table 1).

3.3.4. Subcellular fate of free drug and conjugates

Fig. 8 depicts the comparative formation of lysosomes after treating MCF-7 and MBA-MD-231 cells for 24 h. The fluorescence intensity of dye was found to be similar in case of free GEM, DTX, DTX-GEM, DTX-GLY-GEM and DTX-LYS-GEM as compared to the control cells (without treatment). Whereas, significantly higher fluorescence intensity was observed when the cells were treated with conjugates having PEG as linker, indicative of higher lysosome or endosome formation.

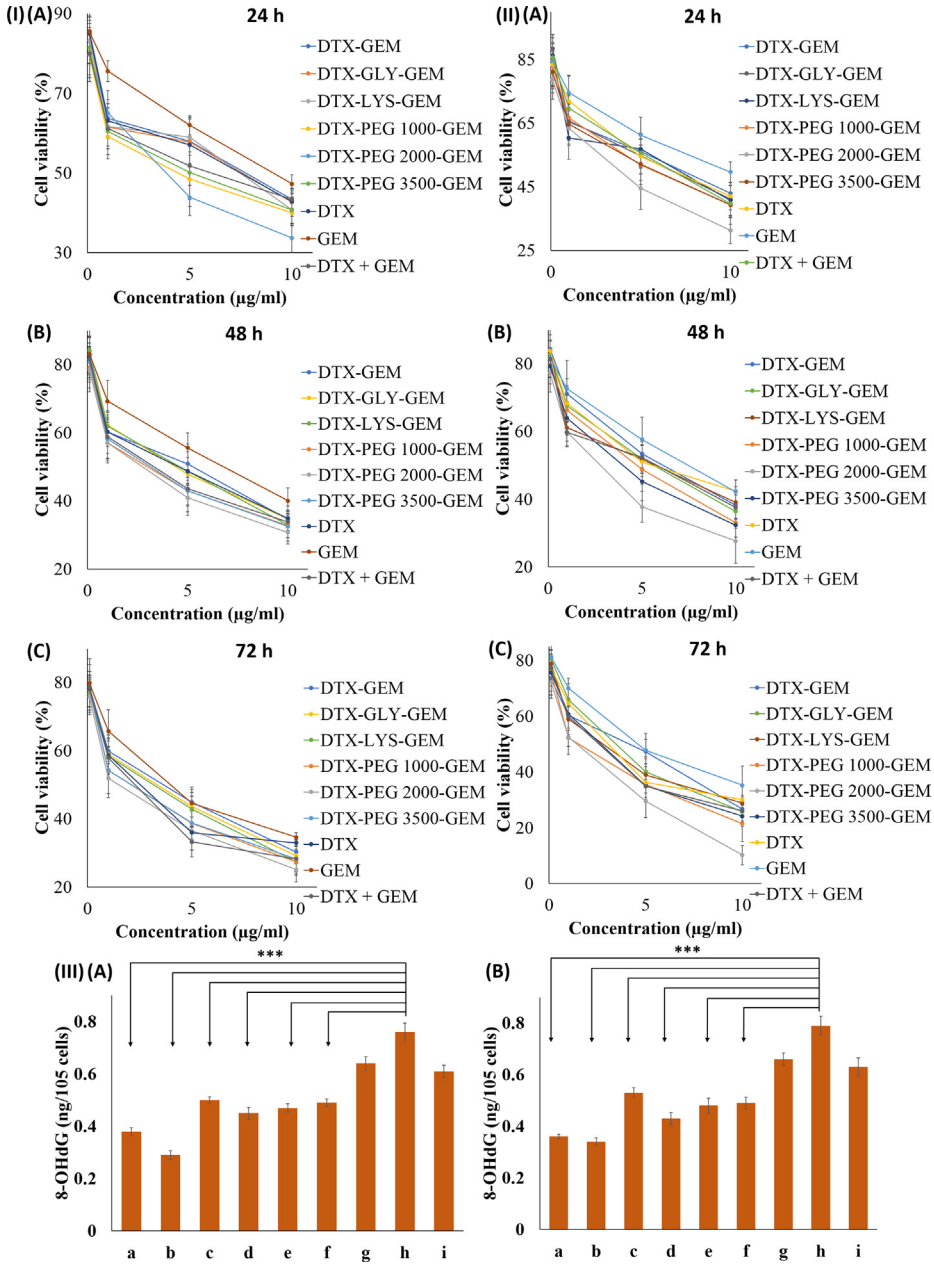

Fig. 7. Concentration and time dependent cell viability of (I) MCF-7 and (II) MDA-MB-231 cells upon treatment with free drugs and conjugates and (III) 8-OHdG levels in (A) MCF-7 and (B) MDA-MB-231 cells treated with (a) free GEM, (b) free DTX, (c) free DTX + GEM (d) DTX-GEM, (e) DTX-GLY-GEM, (f) DTX-LYS-GEM, (g) DTX-PEG1000-GEM, (h) DTX-PEG2000-GEM and (i) DTX-PEG3500-GEM. Values are expressed as Mean ± SD (n = 3). ***, significant difference at $p < 0.001$.

3.3.5. Annexin V apoptosis assay

The observed results of cell cytotoxicity and DNA damage assay were further confirmed by the apoptosis assay in MCF-7 and MDA-MB-231 cell lines (Fig. 9). Apoptosis index in case of long linker conjugates was found to be higher as compared to individual drug, their combination and small linkers in both the cell lines. The apoptotic index was found to be 0.42 and 0.37 in case of GEM while 0.59 and 0.64 in case of DTX against MCF-7 and MDA-MB-231 cell lines, respectively. In line with the results obtained from MTT assay, the DTX-PEG2000-GEM exhibited significantly higher apoptotic index of 0.91 and 0.93 in MCF-7 and MDA-MB-231 cell lines.

3.4. In vivo studies

3.4.1. Pharmacokinetics

Different pharmacokinetic parameters of GEM following *i.v.* administration of the samples is summarized in Table 2. The $AUC_{(0-\infty)}$ value of GEM was found to be 4.21 and 3.81-fold, in case of DTX-PEG3500-GEM and DTX-PEG2000-GEM, respectively, compared with that of GEM, while, the conjugates with zero and short length linker demonstrated slight appreciation in $AUC_{(0-\infty)}$.

3.4.2. Toxicity evaluation

Fig. 11(I) represents different levels of biochemical parameters following the treatment with individual drugs, their combination and different conjugates. Long length linker conjugates demonstrated insignificant difference in the hepato- and nephro-toxicity profile with respect to control. Furthermore, the groups treated with DTX and GEM and their combination exhibited significantly higher ($p < 0.001$) level of AST, ALT and MDA as compared to control. Interestingly, the direct conjugate and short length linker conjugates also demonstrated significantly higher level ($p < 0.001$) of AST, ALT and MDA as compared

Table 1
Effect of inhibitor on cytotoxic activity of free drugs and conjugates in MCF-7 and MDA-MB-231 cell lines.

Samples	MCF-7						
	IC_{50} (Control)	IC_{50} (DIP)	Relative Resistance	IC_{50} (GNT)	Relative Resistance	IC_{50} (CPZ)	Relative Resistance
DTX	4.70 ± 0.31	29.61 ± 0.19	6.30	5.31 ± 0.24	1.13	5.02 ± 0.21	1.07
GEM	9.76 ± 0.56	103.55 ± 1.17	10.60	10.54 ± 0.67	1.08	11.12 ± 0.87	1.14
DTX + GEM	3.19 ± 0.23	25.68 ± 0.14	8.05	3.09 ± 0.14	0.97	3.38 ± 0.16	1.06
DTX-GEM	4.88 ± 0.18	28.24 ± 0.23	5.78	5.95 ± 0.26	1.22	5.80 ± 0.35	1.19
DTX-GLY-GEM	4.46 ± 0.24	27.91 ± 0.15	6.25	5.21 ± 0.19	1.17	5.53 ± 0.29	1.24
DTX-LYS-GEM	4.39 ± 0.28	21.51 ± 0.22	4.89	5.53 ± 0.27	1.26	5.88 ± 0.39	1.34
DTX-PEG1000-GEM	2.58 ± 0.11	2.69 ± 0.13	1.04	9.21 ± 0.57	3.57	14.68 ± 1.07	5.69
DTX-PEG2000-GEM	2.15 ± 0.13	2.05 ± 0.11	1.02	8.25 ± 0.53	3.84	13.37 ± 0.78	6.22
DTX-PEG3500-GEM	3.01 ± 0.18	3.15 ± 0.16	1.04	11.88 ± 0.74	3.95	18.48 ± 1.13	6.14
Samples	MDA-MB-231						
	IC_{50} (control)	IC_{50} (DIP)	Relative Resistance	IC_{50} (GNT)	Relative Resistance	IC_{50} (CPZ)	Relative Resistance
DTX	4.61 ± 0.29	31.68 ± 0.23	6.87	4.88 ± 0.17	1.06	4.47 ± 0.28	0.97
GEM	10.76 ± 0.84	95.14 ± 1.08	8.83	12.37 ± 1.11	1.15	11.40 ± 0.69	1.06
DTX + GEM	2.90 ± 0.22	26.67 ± 0.20	9.17	3.22 ± 0.14	1.11	3.22 ± 0.22	1.11
DTX-GEM	4.65 ± 0.26	29.07 ± 0.16	6.24	5.76 ± 0.21	1.24	5.62 ± 0.21	1.21
DTX-GLY-GEM	4.22 ± 0.17	25.55 ± 0.23	6.05	5.10 ± 0.19	1.21	4.89 ± 0.28	1.16
DTX-LYS-GEM	4.03 ± 0.27	24.91 ± 0.18	6.17	5.04 ± 0.16	1.25	5.28 ± 0.32	1.31
DTX-PEG1000-GEM	3.26 ± 0.15	3.56 ± 0.19	1.08	11.92 ± 0.62	3.65	18.97 ± 1.21	5.81
DTX-PEG2000-GEM	1.70 ± 0.09	1.68 ± 0.11	0.98	6.67 ± 0.33	3.91	10.87 ± 0.72	6.37
DTX-PEG3500-GEM	3.04 ± 0.22	3.12 ± 0.21	1.02	11.80 ± 0.82	3.87	18.44 ± 1.04	6.05

IC_{50} values are mentioned in μg/mL. Values are presented as mean ± SD (n = 3).

to both control and PEGylated conjugates.

In line with the hepatotoxic results, significantly higher ($p < 0.001$) level of BUN and creatinine was observed in the animals treated with DTX and GEM their combination, direct conjugate and short length linked conjugates compared to control and PEGylated conjugate treated animals. However, the increase in the levels of BUN and creatinine in case of DTX treatment was not found to be as prominent as observed in case of GEM and the combination of DTX and GEM (Fig. 11(I) E and F).

The toxicity evaluation via biochemical parameters was further corroborated with histopathological examinations. It is evident from the histological sections of liver, kidney and spleen, that the groups treated with DTX and GEM, their combination, direct conjugate and short length linked conjugates of DTX and GEM exhibited pronounced level of drug induced toxicity, while, the animals treated with PEGylated conjugates demonstrated normal parenchymal cell physiology, in additions, no sign of inflammation and necrosis was observed (Fig. 11(II)). Interestingly, long length linker conjugates, DTX-PEG2000-GEM and DTX-PEG3500-GEM exhibited almost no drug induced hepato- and nephro-toxicity as evident by both histopathological sections and biochemical level estimation.

3.4.3. *In vivo hemolysis*

To access the real time hemolytic side effect of the DTX, GEM and the synthesized conjugates blood samples were collected and processed to separate RBCs and analyzed by SEM. DTX and GEM and their combination exhibited severe alteration in surface morphology of RBCs indicative of hemolytic toxicity (Fig. 12). In line with the *in vitro* hemolysis results, the short and zero length conjugates also elicited the surface roughness and structural changes of RBCs. Interestingly, the animals treated with PEGylated conjugates (long length linked conjugate), did not show any noticeable change as compared to control animals.

4. Discussion

Dual drug conjugates have been reported to enhance the therapeutic efficacy by changing the physicochemical properties and thus the pharmacokinetics of individual drug. For conjugation a variety of linkers and/or direction conjugation have been reported which confuses about the selection of linker or direct conjugation for improved therapeutic performance. Direct conjugation of paclitaxel (PTX) with GEM has been reported to significantly lower the *in vitro* cytotoxicity in comparison with combination of free GEM.HCL and PTX (Aryal et al., 2010). In contrast, we found significantly higher therapeutic efficacy when the GEM was conjugated to methotrexate or curcumin, via long length linkers (Das et al., 2014; Jain et al., 2014b). Different observations in somewhat opposite directions necessitated to investigate the effect of direct conjugation and/or different linkers on the *in vitro* and *in vivo* performance. As far as the present literature is concerned no report is available with detailed investigation in this area. Thus, in the present study, to clarify the unexplored mechanism of the different conjugates towards their biological action, a series of novel bio-conjugates of GEM and DTX with different linker (zero, short and long linker) were synthesized and extensively evaluated for the transformation in physiochemical property and the effect of linker on cellular interaction, cell cytotoxicity and *in vivo* pharmacokinetics.

The selection of DTX and GEM was based on the clinical reports, which demonstrates that the combination of DTX and GEM is well tolerated and active as first-line therapy for advanced, metastatic non-small-cell lung, metastatic uterine leiomyosarcoma and metastatic breast cancer (Fidias et al., 2008; Hensley et al., 2002; Mavroudis et al., 1999). GEM and DTX exhibit distinct mechanisms of action and partially non-overlapping toxicity, thus their combination therapeutic regimen demonstrated synergistic antitumor activity against several different tumour along with lower toxicity. In-addition, conjugation of both drugs will counterbalance the poor physiochemical properties of DTX (extreme hydrophobic) and GEM (extreme hydrophilicity) and will render the necessary hydrophilic–lipophilic balance (HLB) to the conjugate.

The DTX and GEM were interlinked via carbamate bond in case of zero linker conjugate, while carbamate as well as amide bond in case of short and long linked conjugates as these bonds are more chemo enzymatically stable as compared to the ketal, ester and acetal bonds (Carvalho et al., 2000).

The synthesized conjugates were than extensively characterized via ^{1}H NMR, ^{13}C NMR, FTIR and UV spectroscopy. Thermal behaviour of PEGylated conjugates was found similar to that of PEG, which might be

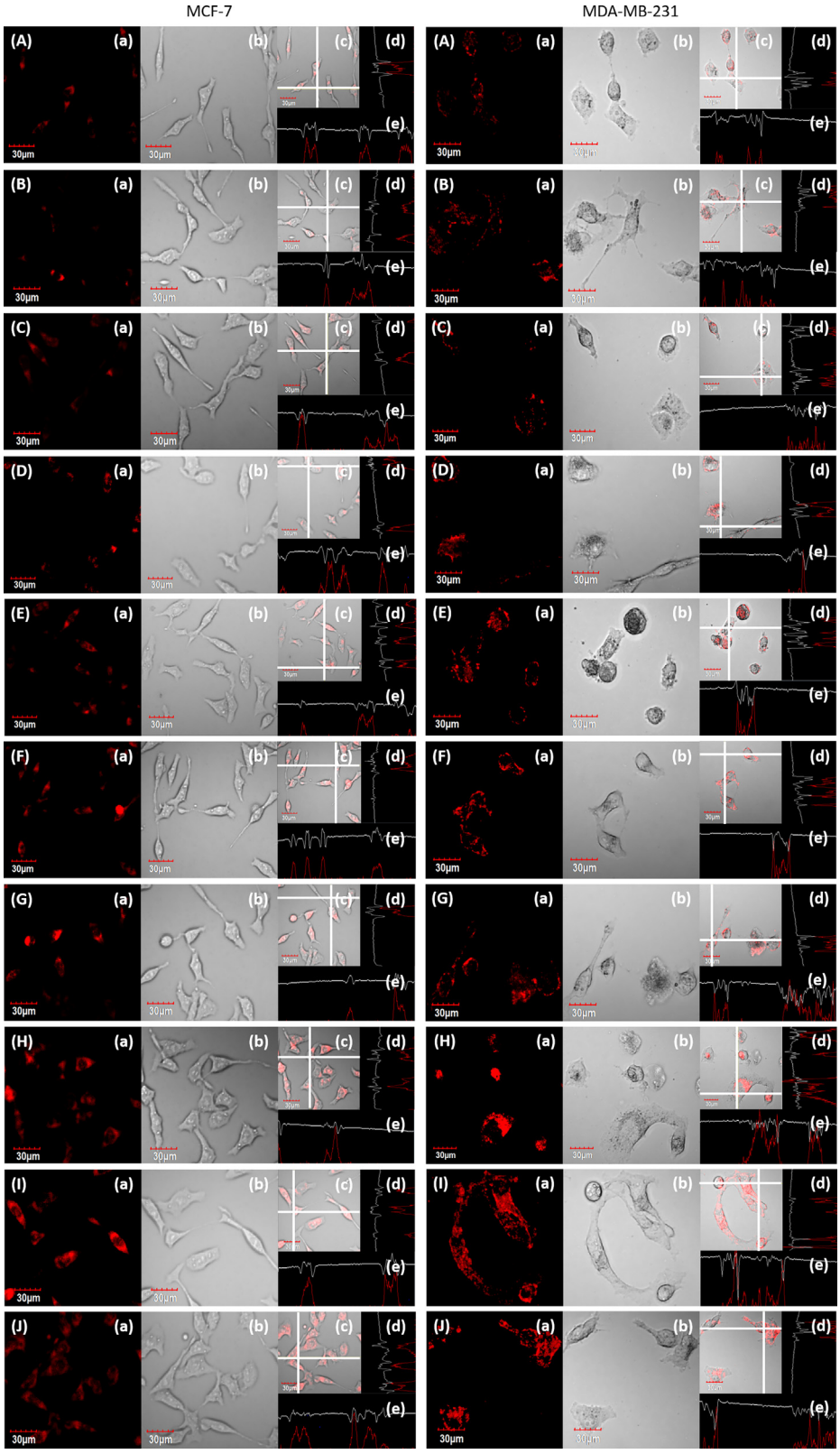

Fig. 8. Intracellular fate of (a) control, (b) free GEM.HCL, (c) free DTX, (d) free DTX + GEM, (e) DTX-GEM, (f) DTX-GLY-GEM, (g) DTX-LYS-GEM, (h) DTX-PEG1000-GEM, (i) DTX-PEG2000-GEM and (j) DTX-PEG3500-GEM shown by staining with LysoTracker Red in MCF-7 and MDA-MB-231 cell lines. (For interpretation of the references to colour in this figure legend, the reader is referred to the web version of this article.)

due to the relatively higher %w/w portion of PEG in the final conjugates. Interestingly, in the case of direct conjugation the melting point was found to be ~150 °C which is very close to DTX, while, the melting point of short and long length linker conjugates was found to be independent of both DTX and GEM, which might be due to the loss of the crystalline structure of drugs following the conjugation. The same trend was noticed in case of solubility of the conjugates, which demonstrates significantly higher solubility of the long length linker

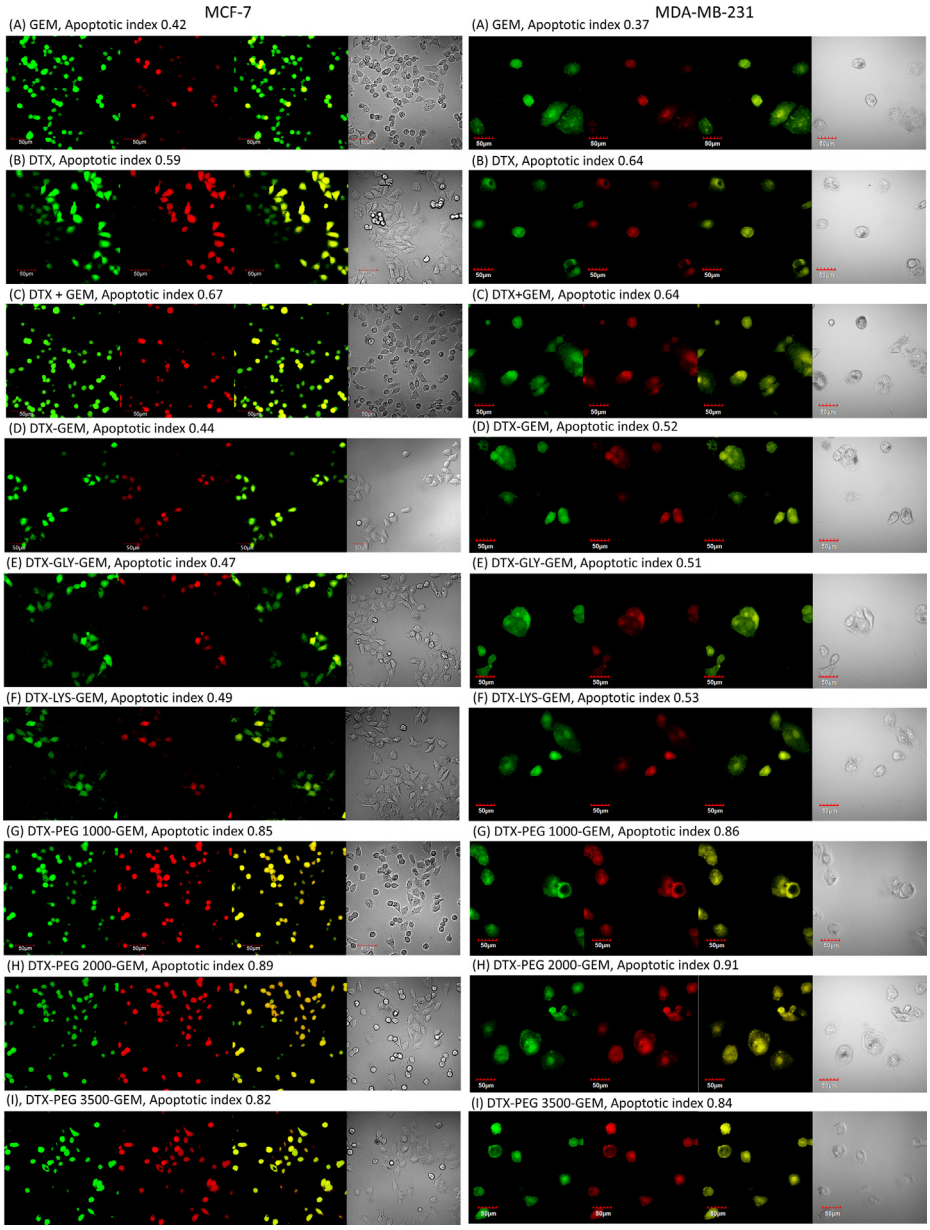

Fig. 9. Apoptosis assay of free drugs and conjugates against MCF-7 and MDA-MB-231 cells; (a) green channel depicts the fluorescence from carboxy fluorescein (cell viability marker dye); (b) red channel depicts fluorescence from Annexin Cy3.18 conjugate (cell apoptosis marker dye) (c) represents the overlay image whereas (d) depicts the differential contrast image of representative cells. The apoptotic index has been measured as the ratio of fluorescence intensity from the red channel to that of the green channel. (For interpretation of the references to colour in this figure legend, the reader is referred to the web version of this article.)

Table 2
Pharmacokinetic parameters of GEM from GEM (10 mg/kg) and conjugates upon *i.v.* administration in rats.

Parameters	GEM	DTX-GEM	DTX-GLY-GEM	DTX-LYS-GEM	DTX-PEG1000-GEM	DTX-PEG2000-GEM	DTX-PEG3500-GEM
C_{30min} (ng/ml h)	1236.6 ± 69.5	813.7 ± 43.2	889.1 ± 41.6	875.4 ± 43.6	955.1 ± 56.8	945.2 ± 61.3	974.7 ± 56.2
$AUC_{(0-24)}$ (ng/ml h)	3673.5 ± 189.9	5424.7 ± 241.2	5381.2 ± 253.2	5006.4 ± 314.1	6896.5 ± 383.2	11531.2 ± 344.8	12506.3 ± 421.4
$AUC_{(0-\infty)}$ (ng/ml h)	4110.5 ± 212.5	6436.1 ± 266.5	6544.2 ± 322.6	6225.3 ± 335.7	10173.7 ± 397.3	15655.4 ± 416.6	17307.6 ± 442.6
$T_{1/2}$ (h)	4.1 ± 0.6	9.15 ± 0.6	9.84 ± 0.7	9.38 ± 0.5	15.4 ± 0.9	24.2 ± 1.2	26.9 ± 1.4

Values are expressed as mean ± SEM (n = 5).

conjugates as compared to free DTX, however, the solubility of PEGylated conjugates was less than that of free GEM, which is the desired outcome to obtain an optimum HLB value. On the other hand, zero and short length linker conjugates exhibits lower water solubility, which might be due to the presence of higher portion of lipophilic DTX in the conjugate.

The conjugates were further analysed for the *in vitro* hydrolysis to understand the effect of different linker on the release behaviour of GEM from the developed conjugates, at pH 7.4 and 5.5, to simulate the systemic circulation and tumor microenvironment, respectively. As evident from the Fig. 5, a sustained release was observed at both the pH conditions, resulting from controlled cleavage of carbamate bond and

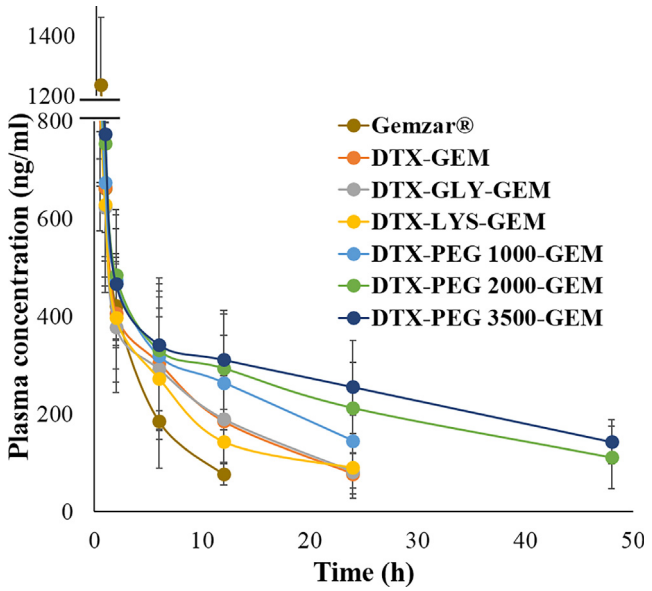

Fig. 10. Plasma concentration–time profiles of GEM and synthesized conjugate following the *i.v.* administration in rats.

both carbamate and amide bond in case of zero, short and long linker conjugates, respectively.

In vitro release study in the presence of protease enzyme demonstrated sustained release of GEM from the conjugates, although, the rate of GEM release was increased in presence of enzyme as compared to simulated media without enzyme. Interestingly, this appreciation in GEM release was more pronounced in case of zero and short length linker conjugates in comparison with long linker conjugates, which might be the result of higher hydrophobicity of zero and short length linked conjugates. Because of high lipophilicity, these conjugates might have higher affinity towards the hydrophobic active domains of enzymes and thus exhibits higher rate of carbamate and amide bond cleavage (Li and Chen, 2006; Makinen et al., 1989). Further, conjugation of DTX and GEM via PEGs, demonstrated higher hydrophilic nature, which is evident from the solubility studies. Steric hindrance towards the enzyme due to the stealth phenomenon of PEG might be the another reason of comparatively lower enzymatic hydrolysis of the conjugates (Borjesson et al., 2007). The conjugates demonstrated higher release of GEM at pH 5.5 (tumor pH) as compared with pH 7.4 (systemic pH), thus, conjugation could be fruitfully exploited to specifically deliver the drugs into the tumor microenvironment.

It is well known that the free GEM is metabolized into 2′,2′-difluorodeoxyuridine (dFdU) when incubated in plasma conditions (via CDA mediated enzymatic degradation) and is the major factor towards lower clinical efficacy of the GEM. Thus, it was of utmost importance to evaluate the role of conjugation on the stability against the enzymatic degradation of GEM. It is clear from the Fig. 6, that the free GEM showed rapid degradation into its inactive metabolite. Whereas, the conjugates with zero and short length linkers demonstrated significantly reduction in the metabolic conversion of GEM via CDA. Sustained release and enhanced protection against CDA mediated degradation could be attributed to the stability of amide or carbamate bond in the conjugates (Moysan et al., 2012). However, the level of dFdU was found to be higher as compared to PEGylated conjugates, which might be due to higher rate of release and lack of stearic hindrance in case of zero and short length linked conjugates. The obtained results were in line with our previous findings which also demonstrated extended plasma stability of GEM conjugates (Das et al., 2014; Jain et al., 2014b; Kushwah et al., 2017; Kushwah et al., 2018a; Kushwah et al., 2018b).

The cell cytotoxicity results revealed significantly higher time and concentration dependent cytotoxicity in both the cell line, when treated with the long length linker conjugate as compared to free drugs, zero and short length linker conjugates. This appreciation in cytotoxicity might be attributed to the presence of additional cellular uptake pathways, ameliorated physicochemical properties of conjugated drugs and improved GEM stability against CDA. Interestingly, the cellular cytotoxicity of the DTX-PEG2000-GEM was found to be slightly higher as compared to DTX-PEG1000-GEM and DTX-PEG3500-GEM, suggesting PEG2000 as an optimum linker for enhancing the therapeutic efficiency of drug-polymer conjugates. In contrast, similar cell inhibition was noticed after treatment of cells with conjugates with zero and short length compared with that of combined therapy of DTX and GEM, which might be due to the lower cell availability of the DTX and GEM following the simple passive diffusion across the cell membranes to the inside of cells bypassing the endocytosis mechanism. Noteworthy, the cytotoxicity of DTX was found to be slightly higher in MDA-MB-231 as compared to MCF-7 cell line, which might be due to the presence of higher OATP1B3 transporters in MDA-MB-231, responsible for internalization of DTX across the cell membrane (Banerjee et al., 2012).

In line with the MTT results, higher levels of 8-OHdG (indicator of oxidative DNA damage) was found, when the cells were treated with long length linker conjugates as compared to free GEM, DTX and their combination, due to higher alteration and oxidative stress mediated by GEM and DTX, respectively (Crea et al., 2011; Isohookana et al., 2015). The results confirmed that the therapeutic efficacy was retained even after conjugation and thereafter the drugs were efficiently transported to the perinuclear and nuclear subcellular regions, after endosomal hydrolytic degradation of amide and carbamate bond.

The internalization of GEM and DTX into the cells requires specialized hNTs (human nucleoside transporters), hENTs (human equilibrative nucleoside transporters), hCNTs (human concentrative nucleoside transporters) and OATPs (organic anion transporting polypeptide) transporters, respectively. Thus, to understand the mechanism and dependency of developed conjugates on hNTs and OATPs for their therapeutic actions, cells were pre-incubated with dipyridamole (hNTs and OATP1B3 inhibitor) before the treatment with conjugates. Following the dipyridamole mediated inhibition of transports, insignificant difference in IC_{50} was observed in case of long length linker conjugates as compared to the control cells (absence of dipyridamole), which might be due to the clathrin mediated endocytic uptake bypassing the transporter dependent cell influx and can be effectively used in overcoming the drug resistance in cancer. Noteworthy, the IC_{50} in case of the free DTX, GEM, zero and short length linked conjugates was significantly increased upon inhibition of transporters with dipyridamole, indicative of OATPs or hNTs mediated transportation of zero and short length linker conjugates. However, the increase in resistance towards DTX was found to be 6.3-fold as compared to 10.6-fold in case of GEM, which might be due to the presence of additional diffusion dependent cell permeation of DTX owing to its hydrophobic nature (Yang et al., 2014). In contrast, increase in IC_{50} of long length linker conjugates was noticed, when the cells were pre-incubated with clathrin and caveolae mediated endocytosis inhibitors as compared to the control cells. The increase in IC_{50} in case of caveolae mediated inhibition was not as prominent as in case of clathrin mediated inhibition, indicating the involvement of both clathrin and caveolae cell uptake mechanism while the clathrin mediated endocytic cellular uptake was the major route for endocytosis. Free drug, zero and short length linker conjugates demonstrated no difference in resistance towards cell cytotoxicity, when preincubated with inhibitors, indicating the involvement of passive diffusion and special transporters as an addition mechanism for cellular uptake.

To further explore the cell uptake mechanism of the developed conjugates, LysoTracker Red dye mediated subcellular trafficking was evaluated. It is evident from Fig. 8, the cells incubated with free DTX, GEM, combination of DTX and GEM, zero and short length conjugates demonstrated insignificant red fluorescence of the LysoTracker Red

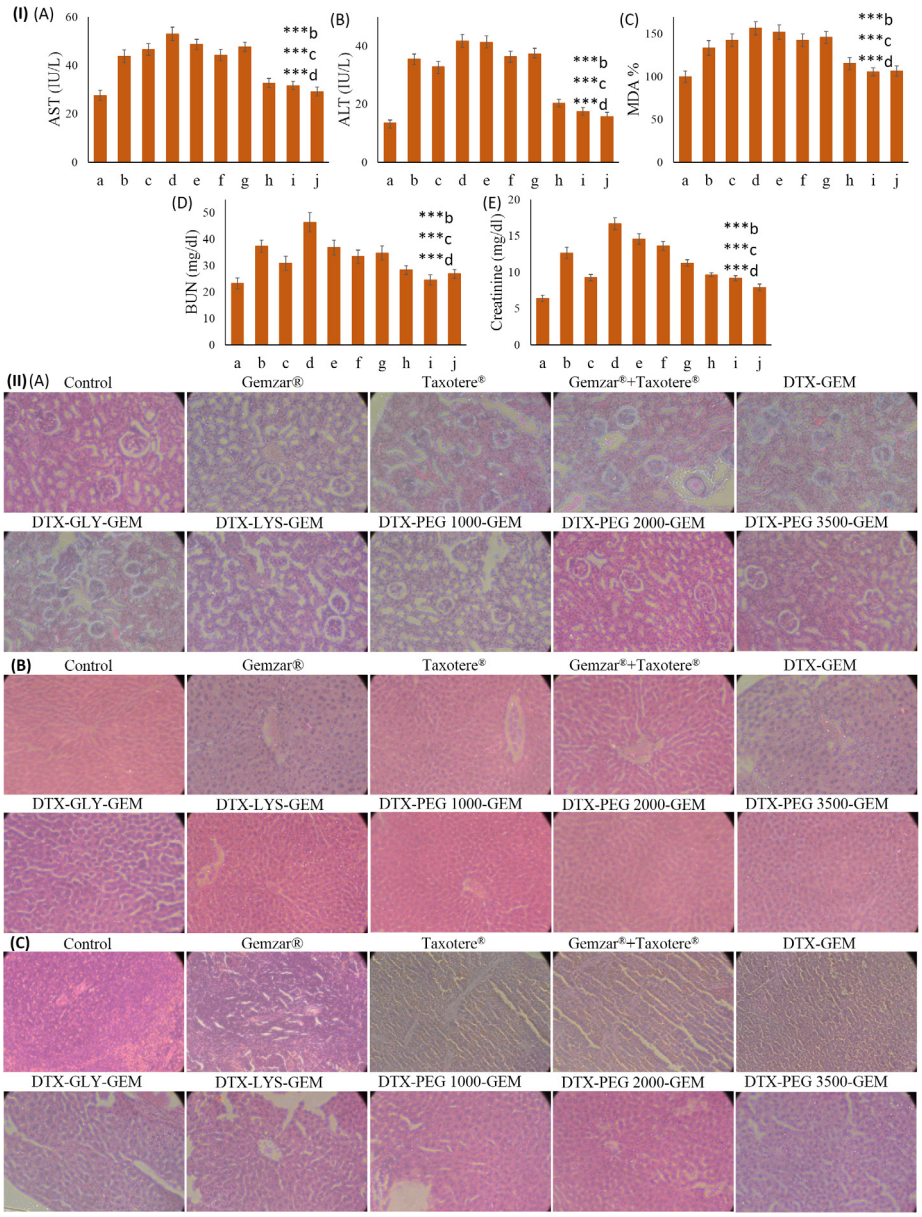

Fig. 11. (I) Biochemical markers (A) AST (B) ALT (D) BUN (E) creatinine levels in plasma and (C) MDA level in liver homogenate after 7 days following administration of (b) GEM, (c) DTX, (d) GEM + DTX (e) DTX-GEM, (f) DTX-GLY-GEM, (g) DTX-LYS-GEM, (h) DTX-PEG1000-GEM, (i) DTX-PEG2000-GEM and (j) DTX-PEG3500-GEM as compared to (a) control. Values are expressed as Mean ± SD (n = 5). ***, significant difference at $p < 0.001$ and (II) Histopathological sections of (A) kidney, (B) liver and (C) spleen following the treatment with different conjugates.

compared to the fluorescence in control cells, while, significantly higher fluorescence was observed when the cells were incubated with long length conjugates. The results clearly indicated substantial increase in the lysosome formation in case of long length linker conjugates in both the cell lines, which further confirm the results obtained from the cell uptake and internalization study, as clathrin mediated endocytic pathway follows endo-lysosome or golgi subcellular structures.

The cell cytotoxicity of the free drugs and synthesized conjugates were further corroborated via apoptosis analysis. The quantitative estimation of apoptosis via Annexin-V assay, demonstrated significantly higher apoptotic index when treated with DTX-PEG2000-GEM as compared to the free drugs, their combination, zero and short length linker conjugates and could be attributed to the higher cell internalization and retention within the cells as compared to plain drug.

The interaction of individual drug(s) and conjugates with the RBCs was analysed in terms of haemolytic activity. It is evident from Fig. S2, the PEGylated conjugates due to stealth property of PEG were devoid of haemolytic activity (Yildirim et al., 2013). On the other hand, severe toxicity was found in case of the DTX and GEM. These results gave further indication that the conjugates exhibited stability against significant conversion into individual drug, responsible of haemolysis and may be safe for the *i.v.* combinatorial therapy of DTX and GEM.

It is well reported in the literature that, the PEGylation improves the circulation time of the drugs via inhibiting the recognition by macrophages and subsequent uptake by reticuloendothelial system (RES). Thus, the effect of different linkers on the *in vivo* pharmacokinetics was assessed (Fig. 10), which revealed significant enhancement in the $AUC_{(0-\infty)}$ value of GEM in case of DTX-PEG2000-GEM as compared to the marketed formulations, zero and short length linked conjugates. Noteworthy, the $AUC_{(0-\infty)}$ value of GEM in case of DTX-PEG3500-GEM was found to be slightly higher even as compared to DTX-PEG2000-GEM, which might be attributed to higher stealth property of PEG3500.

As evident from Fig. 11(I), insignificant ($p > 0.05$) difference in

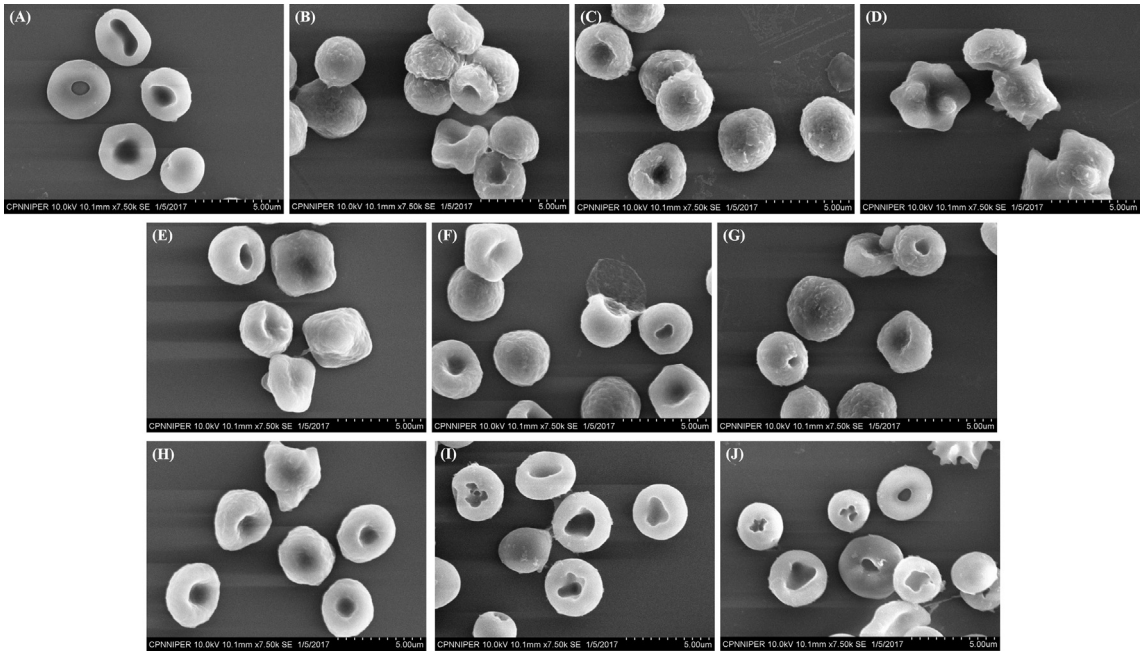

Fig. 12. SEM micrographs of RBCs indicative of (A) control and different groups treated with (B) GEM, (C) DTX, (D) GEM + DTX (E) DTX-GEM, (F) DTX-GLY-GEM, (G) DTX-LYS-GEM, (H) DTX-PEG1000-GEM, (I) DTX-PEG2000-GEM and (J) DTX-PEG3500-GEM.

the AST and ALT levels was observed in case of DTX-PEG3500-GEM and DTX-PEG2000-GEM treated animals in comparison with the control group, revealing enhanced hepatic safety potential of the developed conjugates, owing to absence of any vehicle related toxicity (polysorbate 80 in case of Taxotere®), stealth property by the virtue of PEG and sustained release profile of drug. Insignificant change in MDA levels further confirmed the absence of oxidative stress related toxicity of long length linker conjugates. Interestingly, none of the conjugates of DTX and GEM and DTX exhibited significantly higher levels of BUN and creatinine (marker of nephrotoxicity), however, remarkably higher levels were found in case of GEM and combination of GEM and DTX (Fig. 11(I) D and E).

Significantly lower toxicity profile associated with the administration of PEGylated (PEG2000 and PEG3500) conjugates of DTX and GEM was further established by the histopathological evaluation of liver, kidney and spleen tissues. As clear from the Fig. 11 (II), the DTX, GEM and their combination showed significant toxicity as compared to the control, while, the cellular integrity was maintained and no sign of inflammation was observed in tissues treated with DTX-PEG2000-GEM and DTX-PEG3500-GEM.

In real time *in vivo* hemolytic toxicity study, surface roughness and change in morphology of RBCs was noticed in case of treatment with DTX, GEM and their combination while the long length linker conjugates showed smooth RBCs surface similar to the RBCs isolated from the control animals (Fig. 12). This observation could be attributed to the hydrophilic nature of the conjugates developed by using long length linkers imparted by PEGs. Direct conjugation and short length linker conjugates also demonstrated significant alteration in RBCs morphology which might be attributed to the high hydrophobicity of the conjugates.

Although, the long length linked conjugates, more specifically DTX-PEG2000-GEM and DTX-PEG3500-GEM exhibited significantly lower side effects compared to control animals, it is vital to further evaluate the dose dependent and long-term toxicity to confirm safety potential of the dual drug conjugate.

5. Conclusion

Extensive studies covering the different aspects of the synthesized conjugates revealed superior efficacy of long length linker conjugates. More specifically, conjugates synthesized by using PEG2000 and PEG3500 revealed enhanced pharmacokinetic and reduced toxicity. To further address the unexplored horizons of linkers, future studies such as *in vivo* therapeutic efficacy and dose dependent long term toxicity can be evaluated to establish safe and effective treatment strategy for combination therapy.

Notes

The authors declare no competing financial interest.

Acknowledgement

The authors are thankful to the Director NIPER, James Graham Brown Cancer Center (University of Louisville, KY, USA) and Strathclyde Institute of Pharmacy & Biomedical Sciences (University of Strathclyde, Glasgow, U.K.) for necessary infrastructure and facilities. Varun Kushwah is also grateful to the Council of Scientific and Industrial Research (CSIR), GOI, New Delhi (Grant ID 09/727(0107)/2013-EMR-I), United States-India Educational Foundation, New Delhi (Grant ID PS00218456) and Commonwealth commission in the UK (Grant ID INCN-2015-29) for providing research funding and fellowships.

Appendix A. Supplementary data

HPLC method development and validation for GEM, FTIR of synthesized conjugates, Physicochemical characterization (solubility and melting point) and in-vitro haemolysis. Supplementary data associated with this article can be found, in the online version, at https://doi.org/10.1016/j.ijpharm.2018.07.016.

References

Albertsson, M., Johansson, B., Friesland, S., Kadar, L., Letocha, H., Frykholm, G., Wagenius, G., 2007. Phase II studies on docetaxel alone every third week, or weekly in combination with gemcitabine in patients with primary locally advanced, metastatic, or recurrent esophageal cancer. Med. Oncol. 24, 407–412.

Aryal, S., Hu, C.M., Zhang, L., 2010. Combinatorial drug conjugation enables nanoparticle

dual-drug delivery. Small 6, 1442–1448.
Banerjee, N., Allen, C., Bendayan, R., 2012. Differential role of organic anion-transporting polypeptides in estrone-3-sulphate uptake by breast epithelial cells and breast cancer cells. J. Pharmacol. Exp. Ther. 342, 510–519.
Borjesson, J., Engqvist, M., Sipos, B., Tjerneld, F., 2007. Effect of poly(ethylene glycol) on enzymatic hydrolysis and adsorption of cellulase enzymes to pretreated lignocellulose. Enzyme Microb. Tech. 41, 186–195.
Caron, J., Maksimenko, A., Mougin, J., Couvreur, P., Desmaele, D., 2014. Combined antitumoral therapy with nanoassemblies of bolaform polyisoprenoyl paclitaxel/gemcitabine prodrugs. Polym. Chem. 5, 1662–1673.
Carvalho, E., Francisco, A.P., Iley, J., Rosa, E., 2000. Triazene drug metabolites. Part 17: synthesis and plasma hydrolysis of acyloxymethyl carbamate derivatives of antitumour triazenes. Bioorg. Med. Chem. 8, 1719–1725.
Chan, S., Romieu, G., Huober, J., Delozier, T., Tubiana-Hulin, M., Schneeweiss, A., Lluch, A., Llombart, A., du Bois, A., Kreienberg, R., Mayordomo, J.I., Anton, A., Harrison, M., Jones, A., Carrasco, E., Vaury, A.T., Frimodt-Moller, B., Fumoleau, P., 2009. Phase III study of gemcitabine plus docetaxel compared with capecitabine plus docetaxel for anthracycline-pretreated patients with metastatic breast cancer. J. Clin. Oncol. 27, 1753–1760.
Crea, F., Duhagon Serrat, M.A., Hurt, E.M., Thomas, S.B., Danesi, R., Farrar, W.L., 2011. BMI1 silencing enhances docetaxel activity and impairs antioxidant response in prostate cancer. Int. J. Cancer 128, 1946–1954.
Das, M., Jain, R., Agrawal, A.K., Thanki, K., Jain, S., 2014. Macromolecular bipill of gemcitabine and methotrexate facilitates tumor-specific dual drug therapy with higher benefit-to-risk ratio. Bioconjug. Chem. 25, 501–509.
Dora, C.P., Trotta, F., Kushwah, V., Devasari, N., Singh, C., Suresh, S., Jain, S., 2016. Potential of erlotinib cyclodextrin nanosponge complex to enhance solubility, dissolution rate, in vitro cytotoxicity and oral bioavailability. Carbohydr. Polym. 137, 339–349.
Fidias, P.M., Dakhil, S.R., Lyss, A.P., Loesch, D.M., Waterhouse, D.M., Bromund, J.L., Chen, R., Hristova-Kazmierski, M., Treat, J., Obasaju, C.K., 2008. Phase III study of immediate compared with delayed docetaxel after front-line therapy with gemcitabine plus carboplatin in advanced non-small-cell lung cancer. J. Clin. Oncol. 27, 591–598.
Fidias, P.M., Dakhil, S.R., Lyss, A.P., Loesch, D.M., Waterhouse, D.M., Bromund, J.L., Chen, R., Hristova-Kazmierski, M., Treat, J., Obasaju, C.K., Marciniak, M., Gill, J., Schiller, J.H., 2009. Phase III study of immediate compared with delayed docetaxel after front-line therapy with gemcitabine plus carboplatin in advanced non-small-cell lung cancer. J. Clin. Oncol. 27, 591–598.
Hensley, M.L., Maki, R., Venkatraman, E., Geller, G., Lovegren, M., Aghajanian, C., Sabbatini, P., Tong, W., Barakat, R., Spriggs, D.R., 2002. Gemcitabine and docetaxel in patients with unresectable leiomyosarcoma: results of a phase II trial. J. Clin. Oncol. 20, 2824–2831.
Huang, J.B., Tao, C., Yu, Y., Yu, F.F., Zhang, H., Gao, J., Wang, D., Chen, Y., Gao, J., Zhang, G.Q., Zhou, G.C., Liu, J.J., Sun, Z.G., Sun, D.X., Zou, H., Xu, H., Lu, Y., Zhong, Y.Q., 2016. Simultaneous targeting of differentiated breast cancer cells and breast cancer stem cells by combination of docetaxel- and sulforaphane-loaded self-assembled poly(D, L-lactide-co-glycolide)/hyaluronic acid block copolymer-based nanoparticles. J. Biomed. Nanotechnol. 12, 1463–1477.
Isohookana, J., Haapasaari, K.M., Soini, Y., Karihtala, P., 2015. Keap1 expression has independent prognostic value in pancreatic adenocarcinomas. Diagn. Pathol. 10, 28.
Jain, A.K., Thanki, K., Jain, S., 2014a. Solidified self-nanoemulsifying formulation for oral delivery of combinatorial therapeutic regimen: part I. Formulation development, statistical optimization, and in vitro characterization. Pharm. Res. 31, 923–945.
Jain, S., Jain, R., Das, M., Agrawal, A.K., Thanki, K., Kushwah, V., 2014b. Combinatorial bio-conjugation of gemcitabine and curcumin enables dual drug delivery with synergistic anticancer efficacy and reduced toxicity. RSC Adv. 4, 29193–29201.
Karlgren, M., Vildhede, A., Norinder, U., Wisniewski, J.R., Kimoto, E., Lai, Y., Haglund, U., Artursson, P., 2012. Classification of inhibitors of hepatic organic anion transporting polypeptides (OATPs): influence of protein expression on drug–drug interactions. J. Med. Chem. 55, 4740–4763.
Kushwah, V., Agrawal, A.K., Dora, C.P., Mallinson, D., Lamprou, D.A., Gupta, R.C., Jain, S., 2017. Novel gemcitabine conjugated albumin nanoparticles: a potential strategy to enhance drug efficacy in pancreatic cancer treatment. Pharm. Res. 34, 2295–2311.
Kushwah, V., Katiyar, S.S., Agrawal, A.K., Gupta, R.C., Jain, S., 2018a. Co-delivery of docetaxel and gemcitabine using PEGylated self-assembled stealth nanoparticles for improved breast cancer therapy. Nanomedicine 14, 1629–1641.
Kushwah, V., Katiyar, S.S., Dora, C.P., Kumar Agrawal, A., Lamprou, D.A., Gupta, R.C., Jain, S., 2018b. Co-delivery of docetaxel and gemcitabine by anacardic acid modified self-assembled albumin nanoparticles for effective breast cancer management. Acta Biomater. 73, 424–436.
Leu, K.M., Ostruszka, L.J., Shewach, D., Zalupski, M., Sondak, V., Biermann, J.S., Lee, J.S.J., Couwlier, C., Palazzolo, K., Baker, L.H., 2004. Laboratory and clinical evidence of synergistic cytotoxicity of sequential treament with gemcitabine followed by docetaxel in the treatment of sarcoma. J. Clin. Oncol. 22, 1706–1712.
Li, C.J., Chen, L., 2006. Organic chemistry in water. Chem. Soc. Rev. 35, 68–82.
Li, J., Chen, Y., Zeng, L., Lian, G., Chen, S., Li, Y., Yang, K., Huang, K., 2016. A nanoparticle carrier for co-delivery of gemcitabine and small interfering RNA in pancreatic cancer therapy. J. Biomed. Nanotechnol. 12, 1654–1666.
Lin, N.M., Zeng, S., Ma, S.L., Fan, Y., Zhong, H.J., Fang, L., 2004. Determination of gemcitabine and its metabolite in human plasma using high-pressure liquid chromatography coupled with a diode array detector. Acta Pharmacol. Sin. 25, 1584–1589.
Liu, P., Sun, Y., Wang, Q., Sun, Y., Li, H., Duan, Y., 2014. Intracellular trafficking and cellular uptake mechanism of mPEG-PLGA-PLL and mPEG-PLGA-PLL-Gal nanoparticles for targeted delivery to hepatomas. Biomaterials 35, 760–770.
Mackey, J.R., Mani, R.S., Selner, M., Mowles, D., Young, J.D., Belt, J.A., Crawford, C.R., Cass, C.E., 1998. Functional nucleoside transporters are required for gemcitabine influx and manifestation of toxicity in cancer cell lines. Cancer Res. 58, 4349–4357.
Makinen, P.L., Clewell, D.B., An, F., Makinen, K.K., 1989. Purification and substrate-specificity of a strongly hydrophobic extracellular metalloendopeptidase (gelatinase) from Streptococcus-faecalis (Strain 0g1-10). J. Biol. Chem. 264, 3325–3334.
Mavroudis, D., Malamos, N., Alexopoulos, A., Kourousis, C., Agelaki, S., Sarra, E., Potamianou, A., Kosmas, C., Rigatos, G., Giannakakis, T., Kalbakis, K., Apostolaki, F., Vlachonicolis, J., Kakolyris, S., Samonis, G., Georgoulias, V., 1999. Salvage chemotherapy in anthracycline-pretreated metastatic breast cancer patients with docetaxel and gemcitabine: a multicenter phase II trial. Greek Breast Cancer Cooperative Group. Ann. Oncol. 10, 211–215.
Moysan, E., Bastiat, G., Benoit, J.-P., 2012. Gemcitabine versus modified gemcitabine: a review of several promising chemical modifications. Mol. Pharmaceutics 10, 430–444.
Musumeci, T., Ventura, C.A., Giannone, I., Ruozi, B., Montenegro, L., Pignatello, R., Puglisi, G., 2006. PLA/PLGA nanoparticles for sustained release of docetaxel. Int. J. Pharm. 325, 172–179.
Parhi, P., Mohanty, C., Sahoo, S.K., 2012. Nanotechnology-based combinational drug delivery: an emerging approach for cancer therapy. Drug Discov. Today 17, 1044–1052.
Reddy, L.H., Couvreur, P., 2008. Novel approaches to deliver gemcitabine to cancers. Curr. Pharm. Des. 14, 1124–1137.
Sherman, W.H., Fine, R.L., 2000. Combination gemcitabine and docetaxel therapy in advanced adenocarcinoma of the pancreas. Oncology 60, 316–321.
Sloat, B.R., Sandoval, M.A., Li, D., Chung, W.G., Lansakara, P.D., Proteau, P.J., Kiguchi, K., DiGiovanni, J., Cui, Z., 2011. In vitro and in vivo anti-tumor activities of a gemcitabine derivative carried by nanoparticles. Int. J. Pharm. 409, 278–288.
Sonawane, R., Harde, H., Katariya, M., Agrawal, S., Jain, S., 2014. Solid lipid nanoparticles-loaded topical gel containing combination drugs: an approach to offset psoriasis. Expert Opin. Drug Deliv. 11, 1833–1847.
Swarnakar, N.K., Thanki, K., Jain, S., 2014. Enhanced antitumor efficacy and counterfeited cardiotoxicity of combinatorial oral therapy using Doxorubicin- and Coenzyme Q10-liquid crystalline nanoparticles in comparison with intravenous Adriamycin. Nanomedicine 10, 1231–1241.
Tan, L., Peng, J., Zhao, Q., Zhang, L., Tang, X., Chen, L., Lei, M., Qian, Z., 2017a. A novel MPEG-PDLLA-PLL copolymer for docetaxel delivery in breast cancer therapy. Theranostics 7, 2652–2672.
Tan, L.W., Ma, B.Y., Zhao, Q., Zhang, L., Chen, L.J., Peng, J.R., Qian, Z.Y., 2017b. Toxicity evaluation and anti-tumor study of docetaxel loaded mPEG-polyester micelles for breast cancer therapy. J. Biomed. Nanotechnol. 13, 393–408.
Vandana, M., Sahoo, S.K., 2010. Long circulation and cytotoxicity of PEGylated gemcitabine and its potential for the treatment of pancreatic cancer. Biomaterials 31, 9340–9356.
Vergniol, J.C., Bruno, R., Montay, G., Frydman, A., 1992. Determination of Taxotere in human plasma by a semi-automated high-performance liquid chromatographic method. J. Chromatogr. 582, 273–278.
Xu, Y., Wang, C., Ding, Y., Wang, Y., Liu, K., Tian, Y., Gao, M., Li, Z., Zhang, J., Li, L., 2016. Nanoparticles with optimal ratiometric co-delivery of docetaxel with gambogic acid for treatment of multidrug-resistant breast cancer. J. Biomed. Nanotechnol. 12, 1774–1781.
Yang, Z.Z., Li, J.Q., Wang, Z.Z., Dong, D.W., Qi, X.R., 2014. Tumor-targeting dual peptides-modified cationic liposomes for delivery of siRNA and docetaxel to gliomas. Biomaterials 35, 5226–5239.
Yao, J., Li, Y., Sun, X., Dahmani, F.Z., Liu, H., Zhou, J., 2014. Nanoparticle delivery and combination therapy of gambogic acid and all-trans retinoic acid. Int. J. Nanomed. 9, 3313–3324.
Yildirim, A., Ozgur, E., Bayindir, M., 2013. Impact of mesoporous silica nanoparticle surface functionality on hemolytic activity, thrombogenicity and non-specific protein adsorption. J. Mater. Chem. B 1, 1909–1920.